

# Membrane Potential: Concepts

AJ Moorhouse, UNSW Australia, Sydney, NSW, Australia

© 2016 Elsevier Inc. All rights reserved.

## Introduction

Everything we do, from playing a challenging piano concerto or sprinting in a 100 m race, or even simply walking and breathing and admiring the birds and trees, involves a complex array of muscle activity and sensory inputs all coordinated by the brain and nerves. As we eat and metabolize our food, sleep and grow from fertilization to maturity, our digestive and endocrine systems regulate our bodies and maintain homeostasis under very different environments. Our respiratory and cardiovascular systems provide the energy to maintain our bodily functions. All of these wonderful activities rely on cellular functions that depend on changes in the small voltage difference across the thin plasma membrane that encapsulates all animal cells, the ‘membrane potential.’ This 20–100 mV gradient across our cell membrane is a key component to cell and body function, and a large fraction of our cellular energy is spent on establishing and regulating this transmembrane voltage. In this article, the author reviews the principles of how membrane potentials are generated by the combination of selective membrane permeability and ion electrochemical gradients. Section ‘Introduction’ will provide some basic principles regarding electrical and chemical properties of ions and cell membranes, section ‘Determinants of the Membrane Potential’ will build on this to describe more specifically how membrane potentials arise as a consequence of electrochemical gradients and selective membrane permeability, and section ‘Measuring Membrane Potential and Relative Membrane Permeability’ will review approaches to measure membrane selectivity and membrane potentials, providing some exemplar values from the literature.

## Definitions of Different Types of Membrane Potentials and Related Terminology

The following list defines some of the different types of membrane potentials, and some related terminology. The article assumes familiarity with these terms ([Box 1](#)).

## Physical-Chemical Properties of the Cell Membrane and Physiological Solutions

The membrane potential, like any voltage difference, reflects a different electrical charge from one point to another point. In this case, the uneven charge distribution is across the cell membrane, from the intracellular surface of the membrane to the extracellular surface of the membrane. This arises due to a different concentration of charged ions on each side of the membrane. So an important introductory concept is that in biology, positively charged cations and negatively charged anions contribute to the charge on either side of the cell membrane, and the flow of charge (or current) across the

membrane is carried by the movement of ions across the membrane. To understand this, we first need to review some simple aspects of electricity and of physical chemistry.

A crystal of common table salt, or NaCl, contains Na and Cl atoms bound tightly together in a lattice bound by ionic bonds. The Na atom loses its electron to the Cl atom to give rise to  $\text{Na}^+$  and  $\text{Cl}^-$  ions. When a pinch of salt is placed into water, the ionic bonds are disrupted by electrical interactions between water and the ions, and the salt crystals dissociate into hydrated  $\text{Na}^+$  and  $\text{Cl}^-$  ions, that is the ions surrounded by a shell of water molecules ([Figure 1\(a\)](#)). The water molecules are ‘polar,’ meaning that the distribution of electrons is not evenly spread across the  $\text{H}_2\text{O}$  molecules – the electrons spend more time around the oxygen atom as compared to the two hydrogen atoms. Hence the oxygen in water has a partial negative charge, while the hydrogen atoms have a partial positive charge. Ions are energetically unstable in isolation but are stabilized in solution by being surrounded by water orientated accordingly with  $\text{Na}^+$  ions surrounded or shielded by negative oxygen water molecules, while the  $\text{Cl}^-$  anion is surrounded by water with the positive hydrogen facing the

### Box 1

**Membrane potential ( $V_m$ ):** A difference in voltage across the cell membrane arising due to small difference in the distribution of ions in the intracellular and extracellular solutions. Defined as intracellular voltage with respect to extracellular voltage.

**Resting membrane potential:** The membrane potential during a period when the cell is not active or being stimulated. Typically, a stable, steady-state condition of about  $-80$  to  $-60$  mV. Note however that many cells have an unstable or fluctuating resting  $V_m$  that if in a regular pattern can be called pacemaker activity.

**Action potential:** A basic unit of cell signaling that involves a transient and rapid change in membrane potential. Although the time course and amplitude of this  $V_m$  change varies widely in cells, in many nerve and muscle cells  $V_m$  changes from about  $-70$  mV up to about  $+20$  mV before returning to  $-70$  mV.

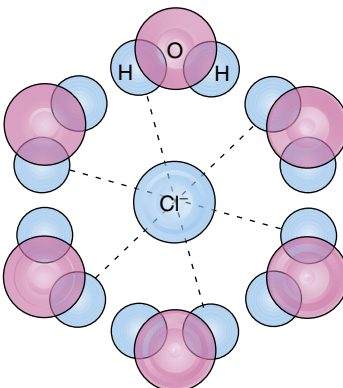
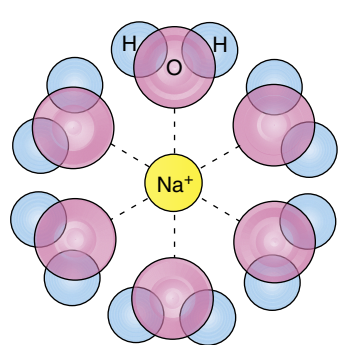
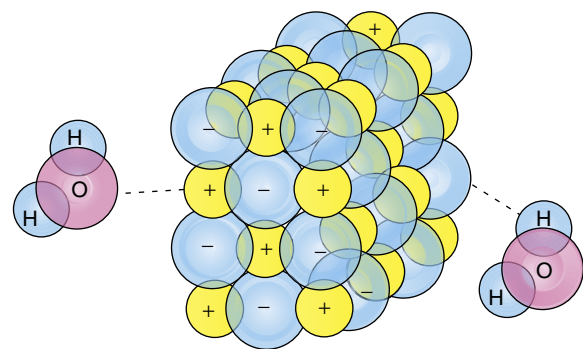
**Depolarization:** A change in the  $V_m$  in a positive direction. Typically increases the probability of a cell firing an action potential, hence typically excitatory.

**Hyperpolarization:** A change in the  $V_m$  in a negative direction. Typically decreases the probability of a cell firing an action potential, hence typically inhibitory.

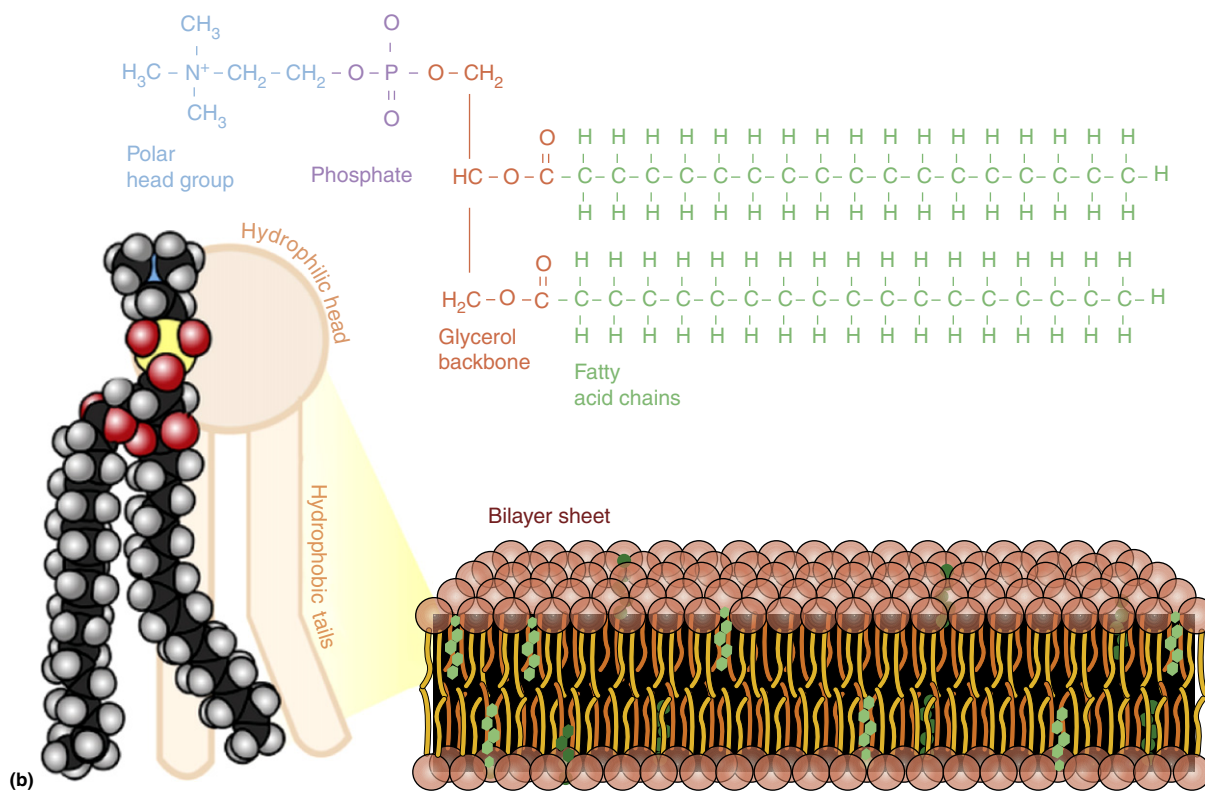
**Repolarisation:** A return of the membrane potential to resting value following a large depolarization, such as the hyperpolarisation phase of the action potential.

**Synaptic potential:** A change in membrane potential in a postsynaptic cell arising from action of a neurotransmitter released by a presynaptic nerve. It can be in the hyperpolarising direction (an inhibitory postsynaptic potential) or in a depolarizing direction (an excitatory postsynaptic potential).

**Sensory potential:** A change in the membrane potential of a sensory receptor neuron arising due to a change in a sensory modality input (touch, smell, taste, vision, and hearing).



(a)



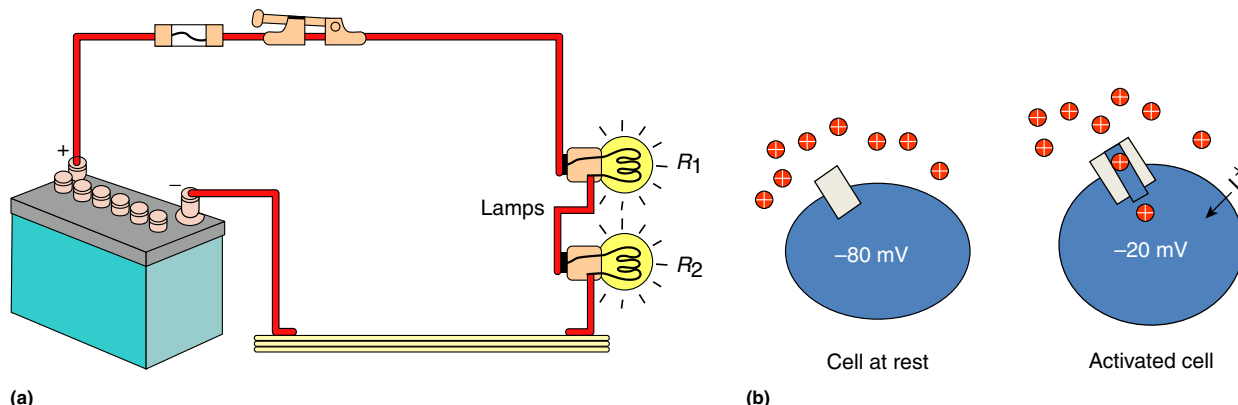


**Figure 2** Electrical circuits: hardwired vs. biology. (a) Schematic diagram of an electrical circuit showing a car battery connected via a wire and switch to two car headlights/lamps. The battery has a different distribution of charges providing a negative and positive pole (cathode and anode, respectively) that drives current in the form of electrons through the wire conductor. Current only flows when the switch is closed to complete the circuit. Current flows through the resistance provided by the lamp filaments, heating the filaments to cause the response – light. Available at: <http://electricalengproject.blogspot.com.au/2012/06/electrical-circuits.html> (accessed 17.02.15). (b) In biology, the electrical battery is equivalent to the membrane potential with a negative charge (cathode) on the inside and a positive charge (anode) outside. When a switch (ion channel) is open, current in the form of charged ions can flow into the cell to cause a response – a depolarization.

anion. Molecules, like ions, that are readily dissolved in water (or become hydrated by water) are said to be 'hydrophilic.'

In contrast to water, the interior of the cell membrane is 'nonpolar' and 'hydrophobic.' The long hydrocarbon chains of the lipid molecules that comprise the membrane have no partial charges and cannot readily dissolve in water. This is readily seen when oil is spilled into water by the way oil forms a film floating on the surface of the water. Nonpolar molecules will however readily interact with other nonpolar molecules (just as polar molecules readily interact). Hence the hydrated ions cannot freely pass through the cell membrane due to this nonpolar lipid core. The energetics of moving an ion from an aqueous solution (with a high dielectric constant of  $\approx 80$ ) to the interior of the lipid bilayer (with a dielectric constant of  $\approx 2$ ) is so high that less than 1 in  $10^{50}$  ions would partition into the membrane (Coster, 2003). The lipid bilayer can therefore readily sustain a charge separation corresponding to a physiological  $V_m$  of  $\pm 100$  mV. As the membrane is only 5–10 nm thick, this corresponds to a very large electric field strength ( $\approx 10^7$  V m $^{-1}$ ), demonstrating the strong insulating capacity of the lipid bilayer. If the  $V_m$  is artificially increased to a few hundred mV, say to 400 mV, the membrane may transiently break down. This 'punchthrough' or dielectric breakdown may become irreversible if even larger voltages are applied across the membrane (1 V or more). The voltage-induced transient membrane rupture has actually been utilized

to enable large molecules to be inserted into the cell by electroporation (Coster, 2009).

If the hydrocarbon tails of lipids are nonpolar, how can they exist bathed by the polar salt solutions that comprise intracellular and extracellular solutions? The answer is that the lipid molecules that make up mammalian cell membranes are phospholipids and ‘amphiphilic,’ containing polar head-groups attached to the nonpolar hydrocarbon tails (**Figure 1 (b)**). The polar headgroups can readily interact with water. These phospholipids will spontaneously adopt a bilayer configuration when placed in a polar solvent such as water – the nonpolar tails will join up and the polar headgroups will form the border with the polar solvent. Hence the plasma membrane of a mammalian cell contains a phospholipid bilayer which physically and electrically separates the intracellular and extracellular solutions. Within this bilayer membrane are inserted numerous proteins which function as membrane transport proteins, enzymes, and receptors to communicate with other cells.

## Electrical Properties of the Cell and Ohm's Law

Consider a simple hardwired electrical circuit such as that found in a hand-held torch or car battery ([Figure 2\(a\)](#)). The driving force for providing electrical current through this

**Figure 1** Schematic structures of hydrated ions and the cell membrane lipids. (a) Schematic diagram of a crystal of common table salt ( $\text{NaCl}$ ; upper panel) with the  $\text{Na}^+$  and  $\text{Cl}^-$  bound in a tight ionic lattice. Upon addition of the polar water ( $\text{H}_2\text{O}$ ) molecule, the  $\text{Na}^+$  and  $\text{Cl}^-$  separate and become hydrated ions (lower panels). Reproduced from Allman, R. A helpful introduction to polar and nonpolar molecules. The chemistry webpages of Robert Allman. Available at: <http://www.chemstone.net/Principles/7.Solutions/Soln.html> (accessed 17.02.15). (b) Schematic diagram of a single typical membrane phospholipid molecule (this example is ‘phosphatidylcholine’) showing its chemical structure and a schematic depiction of its hydrophobic fatty acid tail, and its polar head (phosphate and choline), joined by the glycerol backbone. The lower right panel depicts a lipid bilayer such as that which forms the cell membrane, with the nonpolar tails joined together, and the polar head groups facing the extracellular and intracellular solutions. Figure accessed from the CK-12 Foundation under a creative commons CC BY-NC license (<http://www.ck12.org/biology/Phospholipid-Bilayers/lesson/Phospholipid-Bilayers/>).

circuit illustrated in **Figure 2(a)** is a 12 V battery. A copper wire that connects the two poles of the battery – the cathode and anode – acts as a conductor of the electrical current. The current is movement of charge in the form of electrons traveling along this conductor. The switch is a break in the wire that only allows current to flow when the circuit between the cathode and anode is complete. The resistance of the circuit is determined by factors such as the thickness, length, and conductivity of the wire, and in this case by the properties of the high-resistance filament placed in series in this circuit. When the switch is on, current flows through the circuit driven by the potential difference (voltage) of the battery, and the filament heats up and provides light to mediate the car headlamp or torch's function.

In biology, the principles are just the same but the elements are different (**Figure 2(b)**). The circuit is the flow of current across the membrane. The current is carried by ions flowing through the circuit. The battery providing the driving force for ionic current flow is the 'electrochemical driving force' for the ion that carries the current. This concept is described in more detail below – let us assume for now that the current carrying ion, say  $\text{Na}^+$ , is equally distributed across the membrane and so only the potential difference across the cell membrane, the  $V_m$ , equates to the battery. At a typical resting  $V_m$  of around  $-80 \text{ mV}$ , the cathode (or negative pole) is the intracellular solution and the anode the extracellular solution. The conductors are the membrane transport proteins (ion channels) that traverse the cell membrane. These channels have a central water filled pore that allows the ion to flow across the membrane, and generally also contain small molecular switches or gates that open or close this channel pore. The resistance of this circuit depends on the properties of these ion channels (how many ions they allow to pass) and how many of these ion channels are open in the cell membrane. When the channel gate is open,  $\text{Na}^+$  ions flow into the cell causing a depolarization and activating some cell function (such as triggering an action potential or the release of a neurotransmitter).

In both the biological circuit and the hardwired circuit, the relationship between the potential difference (the battery, voltage,  $V$ ), the amount of current ( $I$ ) flowing through the circuit, and the resistance ( $R$ ) or conductance ( $G$ ) of the circuit is given by 'Ohm's law' (eqn [1]):

$$V = IR = I/G \quad [1]$$

From Ohm's law we can see that when current is injected into a typical cell, for example, by cations entering the cell from the external solution, the extent of the resultant depolarization produced depends on the resistance of the cell. The intracellular salt solution has a very low resistivity, so the cell's resistance depends on the amount of cell membrane, and the resistance of each unit of cell membrane. A cell membrane with a lot of open ion channels has a low resistance (or a high conductance, or is 'leaky') and will generate a smaller voltage change than that of a higher resistance cell in response to the same input of ionic current. Indeed, opening of ion channels to reduce a cell's input resistance and thereby reduce the voltage response to current injection is an important mechanism of inhibition in the brain ('shunting' inhibition; **Farrant and Kaila, 2007**). Given the same distribution of open ion

channels in a cell membrane, a larger cell will have a lower input resistance, and will require a greater input of ionic current to reach a specific  $V_m$  level. A physiological illustration of this is the 'size principle' for motoneuron recruitment during muscle contraction (**Henneman et al., 1965**). At modest levels of ionic current from afferent nerve drive, only the higher resistance smaller motoneurons are depolarized to the voltage threshold and activated. These small motoneurons innervate the 'slow-twitch' type muscle fibers that produce only modest muscle force. When stronger muscle contractions are needed, a greater afferent drive is needed to depolarize and activate the larger motoneurons that supply the fast twitch, high-force fibers. Hence by recruiting motoneurons in order of size and force, the brain can control the extent of motor force needed for a task (increasing force by increasing the frequency of activation is also important).

Ohm's law illustrates a very simple circuit with current flowing through a resistor driven by a voltage gradient. However, the cell membrane behaves like a resistor and a capacitor in parallel (**Figure 3**). A capacitor is an electrical device designed to store charge, and consists of two conducting plates separated by insulating material. The conducting plates are the salt solutions, and the insulating material is the lipid core. The lipid can support a different distribution of charges, or a different potential on each side. In a perfect capacitor, this charge separation would be maintained without decrement. However, the cell membrane contains ion channels that act as a resistor to allow the flow of charge (current) across the membrane. Therefore, the membrane is like a leaky capacitor. When charge is moved from one side to the other, via ionic current flow through open ion channels, the voltage on the two plates of the capacitor (the intracellular and extracellular surface) starts to change, but the change in  $V_m$  is not instantaneous. Current flows through the capacitive element of the circuit as the voltage across the capacitor changes. A new voltage difference is eventually established across the membrane, with an amplitude dependent on the membrane current,  $I_m$  and the membrane resistance,  $R_m$ , as given by Ohm's law. Although the current is applied virtually instantaneously as ion channels rapidly open and close, the change in  $V_m$  changes with a membrane time constant ( $\tau$ ), given by the product of the resistance and capacitance of the circuit. **Figure 3** demonstrates the electrical circuit equivalent for a cell membrane, and the time course of a change in  $V_m$  when current flows into a cell.

## Determinants of the Membrane Potential

The membrane potential ( $V_m$ ) arises due to a different distribution of ions on each side of the membrane. One needs to understand two broad concepts to appreciate how this different distribution of ions can occur. Firstly, one needs to appreciate the forces that determine whether an ion moves in or out of the membrane. Secondly, there needs to be a means by which ions can move across the membrane – the membrane needs to be permeable to that ion. In this section we describe these two factors that determine the distribution of ions across the membrane, and thereby determine the  $V_m$ .

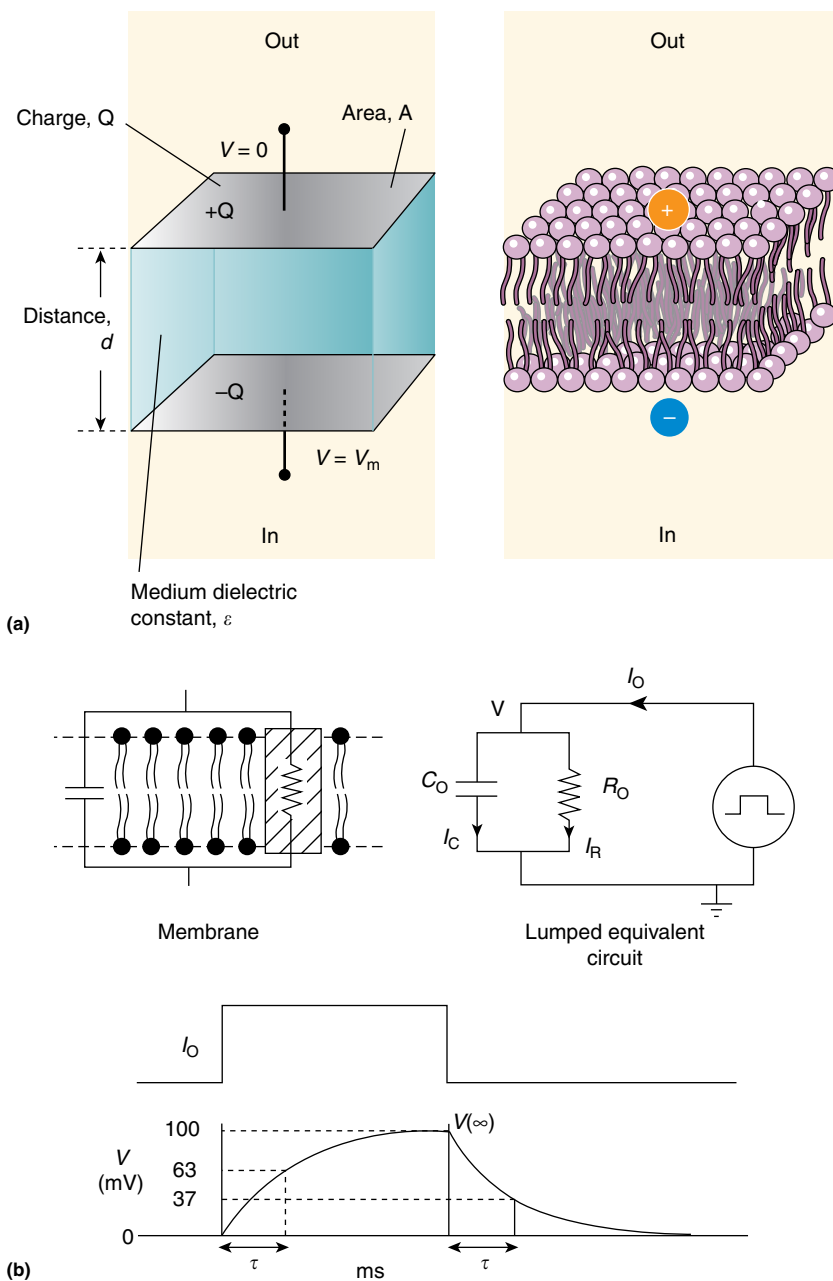


**Figure 3** Electrical equivalent and voltage response of the cell membrane. (a) The lipid bilayer (right) acts like an ideal capacitor (left) that separates a charge,  $Q$ , on the two conducting plates, separated by a distance,  $d$ . The charge separation gives rise to a Voltage ( $V$ ) across the capacitor ( $C$ ), related by the equation  $Q=CV$ . The capacitance is directly proportional to the area of the plates,  $A$ , the dielectric constant of the medium,  $\epsilon$ , the permittivity constant  $\epsilon_0$ , and inversely proportional to the distance between the plates ( $C=A\epsilon_0\epsilon/d$ ). (b) The membrane behaves electrically as an 'RC' circuit, an electrical circuit with a capacitor (from the lipid bilayer) and a resistance (from the ion channels) in parallel. Injection of a square pulse of current into this circuit (as may happen when an ion channel opens) gives rise to a slowly rising and decaying change in voltage as shown in the lower panel. The current rises to a value of  $V=IR$  with a time course dependent on  $\tau$ , the membrane time constant ( $=RC$ , or the time to decay to 37% of maximum, = the time to reach 63% of maximum). The voltage at time,  $t$ , during the rising phase is given by  $V_t=IR \times (1-e^{-t/\tau})$  while the voltage at any time,  $t$ , during the decay phase is given by  $V_t=IR \times e^{-t/\tau}$ . Panel (a) is reproduced from panel C of Figure 6.9 in Boron, W.F., Boulpaep, E.L., 2009. Medical Physiology. A Cellular and Molecular Approach, second ed. Philadelphia, PA: Saunders Elsevier, © 2002 Elsevier Science, USA; Panel (b) with permission from Prof. Peter Barry, © PH Barry, 2002.

### Electrochemical Driving Force for Ion Movement

The major ionic species inside and surrounding cells are  $K^+$ ,  $Na^+$ , and  $Cl^-$ . Larger molecules that carry negative charges,

such as proteins and organic anions, and that find it difficult to cross the membrane form a pool of impermeant anions inside cells. Smaller concentrations of other ions such as bicarbonate,  $Ca^{2+}$ , inorganic phosphates ( $H_2PO_4^-$ ,  $HPO_4^{2-}$ ), and  $Mg^{2+}$

**Table 1** Physiological concentrations and equilibrium potentials of common physiological electrolytes

Ion	Extracellular (mM)	Intracellular (mM)	$E_{ion}$ (mV; 37 °C)	$V_m - E_{ion}$ (mV)	Gradient at rest
Na <sup>+</sup>	145	18	+ 56	- 132	Influx
K <sup>+</sup>	3.0	135	- 102	+ 26	Efflux
Ca <sup>2+</sup>	1.2	10 <sup>-7</sup>	+ 125	- 201	Influx
Cl <sup>-</sup>	120	7	- 76	0	Nil
HCO <sub>3</sub> <sup>-</sup>	23	15	- 11	- 65	Efflux
pH [H <sup>+</sup> ]	7.4	7.2	- 12	- 64	Influx
Osmolality	290	290	Not applicable	Not applicable	Nil H <sub>2</sub> O gradient

Note: Concentrations of Na<sup>+</sup>, K<sup>+</sup>, Ca<sup>2+</sup>, and Cl<sup>-</sup> are based on McCormick (2008); [HCO<sub>3</sub><sup>-</sup>] which was calculated using the Henderson–Hasselbalch equation (pH = 6.1 + log [HCO<sub>3</sub><sup>-</sup>] – log (0.031 × PCO<sub>2</sub>)) using the given pH values, and with CO<sub>2</sub> = 5% (PCO<sub>2</sub> = 38 mmHg).  $E_{ion}$  calculated for 37 °C using concentrations, assuming equal activities in both solutions. Resting  $V_m$  was taken as - 76 mV, as measured for hippocampal neurons *in vivo* by Tyzio *et al.* (2008).

also exist in the extracellular and intracellular solutions. These ions do not exist in equal concentrations in these two solution compartments. **Table 1** lists the brain concentrations of some physiological ions important in the context of membrane potentials. Cells use a significant amount of energy to actively transport or ‘pump’ ions across the membrane to establish these different concentrations. The Na<sup>+</sup> pump, for example, hydrolyzes adenosine triphosphate (ATP) to pump Na<sup>+</sup> ions out of the cell and to pump K<sup>+</sup> ions into the cell (reviewed in Kaplan, 2002). The Na<sup>+</sup> pump is one of the most important proteins in our bodies and found in virtually all polarized mammalian cells, where it creates a concentration gradient for K<sup>+</sup> and Na<sup>+</sup> across the cell membrane. The Law of Diffusion dictates that substances move from high to low concentrations, as the thermal motions of molecules give rise to collisions between closely spaced molecules that drives them further apart. Hence a chemical force exists for ions to move across the membrane from a high concentration to a low concentration. The chemical force acts to move K<sup>+</sup> from the intracellular solution to the extracellular solution, and to move Na<sup>+</sup> from extracellular to intracellular solution. However, as ions are charged substances, they are also subject to electrical forces. When placed in an electric field, a cation will be attracted to the negative pole and repelled from the positive pole, another Law of Physics – opposite charges attract and like charges repel. The cell membrane potential is an electric field across the membrane, and hence will also attract and repel ions from its positive and negative poles. The next paragraph examines how these two forces combine to produce a specific  $V_m$ .

Consider a hypothetical cell (**Figure 4**) in which the Na<sup>+</sup> pump has established concentration gradients for Na<sup>+</sup> and K<sup>+</sup> across the cell membrane. This hypothetical cell is simplified by balancing the positive charge of these cations by including equimolar concentrations of Cl<sup>-</sup> on both sides. At hypothetical time = 0 the membrane does not allow any ions to cross – it is impermeant to all the ions. The ionic charges are balanced in both the inside solution and outside solution (**Figure 4(a(i))**). Let us now make the membrane permeable to K<sup>+</sup> by including open K<sup>+</sup> – selective ion channels in the membrane. These channels we assume to be perfectly selective for K<sup>+</sup>, so the membrane remains impermeant to Cl<sup>-</sup> and Na<sup>+</sup>. The K<sup>+</sup> ions will diffuse down their concentration gradient, from inside to out, carrying their positive charge as they move across the membrane. Their diffusion results in an excess

of K<sup>+</sup> on the extracellular side of the membrane, and a deficit of K<sup>+</sup> on the intracellular side. There exists an uneven distribution of charges, and hence the membrane is now polarized; negatively charged on the inside with respect to the extracellular side (**Figure 4(a(ii))**). This provides an electrical force on the ions. The negative  $V_m$  acts to attract the K<sup>+</sup> toward the intracellular solution, countering the effects of the chemical force. An electrochemical equilibrium will be reached, where the chemical and electrical forces are equal, and the efflux of K<sup>+</sup> due to the concentration gradient will be balanced by equal influx of K<sup>+</sup> attracted by the negative  $V_m$ . The  $V_m$  at which this equilibrium is reached is called the equilibrium potential ( $E_{ion}$ ) or Nernst potential. The Nernst equation (**Box 2** below) equates the electrical and chemical forces that act on a specific ion, and is used to calculate the equilibrium potential for each specific ion (**Table 1**).

### Relative Membrane Permeability

As shown in **Table 1**, the equilibrium potential for K<sup>+</sup> under physiological ion concentrations in the brain and at body temperature is about - 100 mV. Hence, if only highly selective K<sup>+</sup> channels were open in a cell the  $V_m$  would rapidly equilibrate at - 100 mV (**Figure 4(b(i))**). Imagine that (**Figure 4(b(ii))**) highly selective Na<sup>+</sup> channels were opened instead of the K<sup>+</sup> channels. Na<sup>+</sup> would flow into the cell down its concentration gradient, causing an excess of positive Na<sup>+</sup> inside the cell and a deficit outside the cell. The membrane would again become polarized with a positive  $V_m$ , that provides an electrical force to oppose the further influx of Na<sup>+</sup>. An electrochemical equilibrium would again be established, but this time at a positive  $V_m$ . The  $V_m$  would reach the equilibrium potential of Na<sup>+</sup> which under typical physiological conditions would be about + 60 mV (**Table 1**). Similarly, if a cell only allows Ca<sup>2+</sup> or Cl<sup>-</sup> to move across the membrane the  $V_m$  would equal the equilibrium potentials of these ions, being + 123 mV or - 76 mV at the physiological concentrations of these ions (**Table 1**).

Imagine now (**Figure 4(b(iii))**) that a hypothetical cell was permeable to both K<sup>+</sup> and Na<sup>+</sup> (and no other ions) and contained physiological ion concentrations as in **Table 1**. K<sup>+</sup> would leave the cell according to the chemical force, causing a negative  $V_m$ , and would continue to leave until the  $V_m$  reached the K<sup>+</sup> equilibrium potential ( $E_K$ , - 102 mV). At the same time, Na<sup>+</sup> would enter, driving the  $V_m$  positive, and would

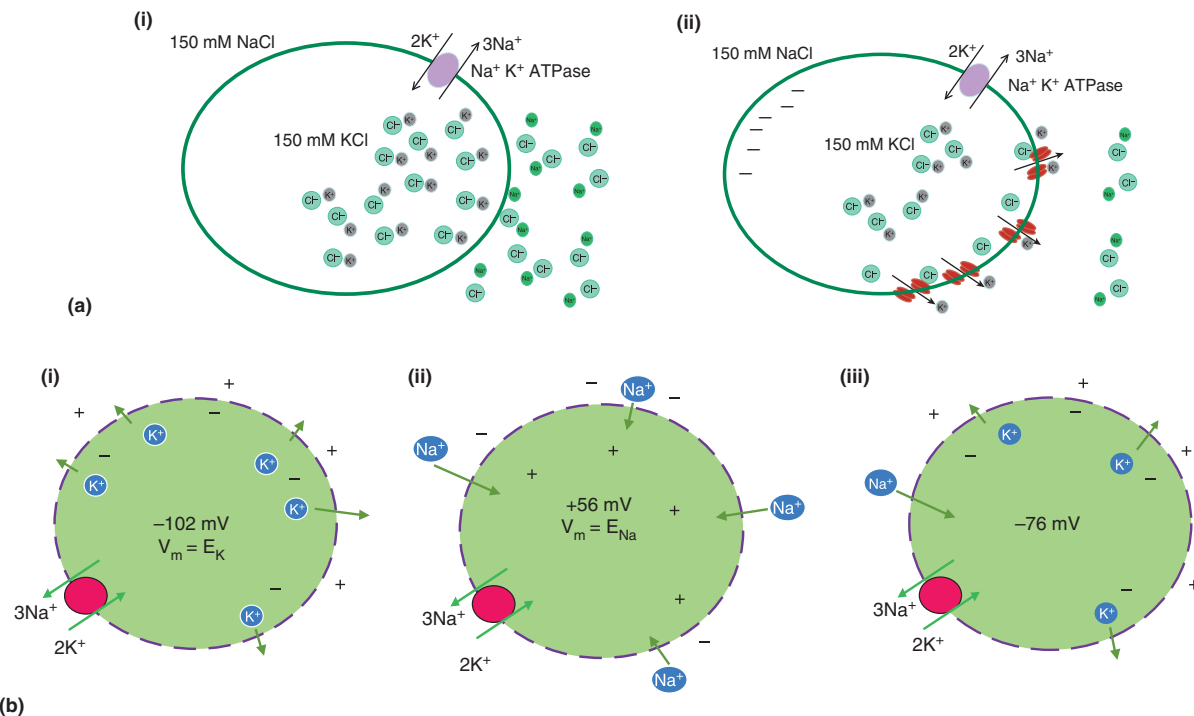


**Figure 4** Electrochemical equilibrium and the resting membrane potential. (a) Schematic diagram illustrating how chemical and electrical forces combine to generate a membrane potential. In panel (i) (left) a hypothetical cell has a  $\text{Na}^+$  pump that establishes concentration gradients for  $\text{Na}^+$  and  $\text{K}^+$ . In (ii) the cell becomes permeable to  $\text{K}^+$ , which flows down its concentration gradient to establish the different ion charge distribution that is the membrane potential ( $V_m$ ). (b) Hypothetical cells as in (a). In (i) only  $\text{K}^+$  is permeable,  $\text{K}^+$  flows out of the cell until the  $V_m$  reaches  $-102 \text{ mV}$ , the equilibrium potential for  $\text{K}^+$  ( $E_K$ ). In (ii) only  $\text{Na}^+$  is permeable,  $\text{Na}^+$  flows in to the cell until the  $V_m$  reaches  $+56 \text{ mV}$ ,  $E_{\text{Na}}$ . In (iii) both  $\text{K}^+$  and  $\text{Na}^+$  are permeable, with  $P_K \gg P_{\text{Na}}$ ,  $\text{K}^+$  flows out of the cell to drive  $V_m$  toward  $E_K$ , while  $\text{Na}^+$  flows in to drive  $V_m$  toward  $E_{\text{Na}}$ . The  $V_m$  reaches a steady-state value somewhere in between, depending on the relative permeability toward  $\text{K}^+$  and  $\text{Na}^+$ . Neither ion is in equilibrium, so continue to flow down their electrochemical energy gradients, but the charge movement of  $\text{Na}^+$  influx is balanced by that from  $\text{K}^+$  efflux. This is similar to the resting  $V_m$  condition in many cells.

continue to enter until  $V_m$  reached the  $\text{Na}^+$  equilibrium potential ( $E_{\text{Na}} + 56 \text{ mV}$ ). The membrane potential would reach some steady-state value that balances these two opposing electrochemical driving forces. The exact value of the  $V_m$  would depend on the relative permeability of the membrane to  $\text{K}^+$  and  $\text{Na}^+$ . If the membrane was mostly permeable to  $\text{K}^+$  ( $P_K \gg P_{\text{Na}}$ ), the  $V_m$  would be closer to  $-100 \text{ mV}$ ; if mostly permeable to  $\text{Na}^+$  ( $P_{\text{Na}} \gg P_K$ ) the  $V_m$  would be closer to  $+60 \text{ mV}$ . If the membrane was equally permeable to both  $\text{K}^+$  and  $\text{Na}^+$  ( $P_K = P_{\text{Na}}$ ), the  $V_m$  would reach a steady-state value half way between  $E_K$  and  $E_{\text{Na}}$  (about  $-20 \text{ mV}$ ). Hence the  $V_m$  is a balance of the electrochemical driving forces for physiologically relevant ions, and the extent to which the membrane is permeable to each of these ions. This can be expressed mathematically using the Goldman-Hodgkin-Katz (GHK) equation (eqn [2]; [Hodgkin and Katz, 1949](#)). For further discussion of GHK and electrodiffusion equations applied to membrane potentials, see [Hodgkin and Katz \(1949\)](#), [Keramidas et al. \(2004\)](#), and/or [Barry \(2006\)](#). If the membrane is only permeable to a single ion, the GHK equation reduces to the Nernst equation.

$$V_m = RT/F \ln \left\{ \frac{P_{\text{Na}}[\text{Na}^+]_{\text{out}} + P_K[\text{K}^+]_{\text{out}} + P_{\text{Cl}}[\text{Cl}^-]_{\text{in}}}{P_{\text{Na}}[\text{Na}^+]_{\text{in}} + P_K[\text{K}^+]_{\text{in}} + P_{\text{Cl}}[\text{Cl}^-]_{\text{out}}} \right\} \quad [2]$$

$$V_m = RT/F \ln \left\{ \frac{[\text{Na}^+]_{\text{out}} + P_K/P_{\text{Na}}[\text{K}^+]_{\text{out}}}{[\text{Na}^+]_{\text{in}} + P_K/P_{\text{Na}}[\text{K}^+]_{\text{in}}} \right\} \quad [3]$$

$$V_m = RT/F \ln \left\{ \frac{[\text{Na}^+]_{\text{out}} + r.P_K/P_{\text{Na}}[\text{K}^+]_{\text{out}}}{[\text{Na}^+]_{\text{in}} + r.P_K/P_{\text{Na}}[\text{K}^+]_{\text{in}}} \right\} \quad [4]$$

**Equations [2]–[4].** The GHK equation expressing the membrane potential ( $V_m$ ) in terms of the permeabilities ( $P_x$ ) for the most prevalent ions in physiological solutions ( $\text{Na}^+$ ,  $\text{K}^+$ , and  $\text{Cl}^-$ ).  $R$ ,  $T$ , and  $F$  have their usual meaning and values as in [Box 2](#). The subscripts in and out refer to intracellular and extracellular concentrations (or more correctly activities). The permeability constants give the velocity of ion movement through the membrane (cm per sec) and depend on the mobility and solubility of the ions in the membrane.  $P_{\text{Na}}$ , for example,  $= RT/Fa \times v_{\text{Na}} \times K_{\text{Na}}$ , where  $a$  = membrane thickness,  $v_{\text{Na}}$  = the mobility of the ion within the membrane, and  $K_{\text{Na}}$  is the partition coefficient between the membrane and aqueous solution. Assuming the membrane is only permeable to  $\text{Na}^+$  and  $\text{K}^+$  (a close approximation for a nerve axon) or that  $\text{Cl}^-$  is passively distributed (so  $E_{\text{Cl}} = V_m$  example in some skeletal muscle fibers) then eqn [2] can be reduced to eqn [3] where  $P_{\text{Na}}/P_K$  is the relative  $\text{Na}^+$  to  $\text{K}^+$  permeability, a parameter that can be more readily

## Box 2 Nernst potential and its derivation

The Nernst potential is derived considering the energy of ions inside and outside the cell at equilibrium – a special situation where there is no energy gradient between inside and outside. The free energy of a mole of ions includes components related to the chemical energy of the ion, the electrical energy acting on the ion and the standard energy on the ion in the absence of applied electrical or chemical energies, a property inherent to each ion species. This can be expressed as:

$$\mu_x = RT \ln[A_x] + zFV + \mu_0^X + PV_n$$

where  $\mu_x$ =the free energy of the ion X,  $R$ =the gas constant (8.314 J K<sup>-1</sup> mol<sup>-1</sup>, Joules per Kelvin per mole (as 1 V=1 JC<sup>-1</sup>, R can also be expressed in terms of VC per K<sup>-1</sup>mol<sup>-1</sup>)),  $T$ =temperature in Kelvins (K=°C+273.15), A is the activity of ion X (which is related to molar concentration, C, by an activity coefficient, γ, specific for a particular salt solution: A=γ.C), ln is the natural logarithm, z is the valency of the ion, F is Faraday's constant (96 485 C mol<sup>-1</sup>, Coulombs per mole), V is the electrical potential (volts, or J C<sup>-1</sup>),  $\mu_0^X$  is the standard state potential for ion x, P is the hydrostatic pressure, and  $V_n$  is the volume of solution occupied by 1 mol of ions, the partial molar volume.

At equilibrium, the free energy of an ion on the outside will equal that of the ion on the inside of the cell so that:

$$\mu_x \text{ outside} = \mu_x \text{ inside}; \text{ or}$$

$$(RT \ln[A_x] + zFV + \mu_0^X + PV_n)_{\text{outside}} \\ = (RT \ln[A_x] + zFV + \mu_0^X + PV_n)_{\text{inside}}$$

The standard state potential is the same inside and outside so can be deleted from both sides. The hydrostatic component is very small in animal cells (but can be large in plant cells) compared to the electrical and chemical forces on the ions (and is also roughly the same on both sides) so can also be eliminated from the equation. The activity coefficient for NaCl (0.75) is very similar to KCl (0.74) when the ionic strength of the intracellular and extracellular solutions are both at physiological values (~0.15 M; see, e.g., [Barry et al., 2013](#)) and so can be eliminated from the equation and activity can be replaced by concentration.

So, after simplification and rearranging, our equation for the transmembrane ion energy difference at equilibrium becomes:

$$RT \ln[C_x]_{\text{outside}} - RT \ln[C_x]_{\text{inside}} = zFV_{\text{inside}} - zFV_{\text{outside}} \text{ or} \\ zF(V_{\text{inside}} - V_{\text{outside}}) = RT \ln[C_x]_{\text{outside}} / [C_x]_{\text{inside}} \text{ or} \\ zFV_m = RT \ln[C_x]_o / [C_x]_i$$

where  $V_m$  is the membrane potential defined as the inside potential relative to the outside potential, and the subscripts o and i refer to outside and inside, respectively.

This is the Nernst equation, where  $V_m$  is the membrane potential where ion X is at electrochemical equilibrium, often referred to as the Nernst potential or Equilibrium potential ( $E_x$ ). In other words,  $V_m$  is the potential at which the chemical and electrical forces on an ion are exactly balanced.

experimentally measured. Equation [4] includes a coupling coefficient, r, to account for the contribution of the electrogenic Na<sup>+</sup> pump (see text).

### Steady State versus Electrochemical Equilibrium – the ‘Resting’ Membrane Potential

In most excitable or polarized cells (e.g., [Figure 4\(b\(iii\)\)](#)), the resting  $V_m$  is about -70 mV, as the membrane permeability is dominated by K<sup>+</sup> relative to other physiological electrolytes.

This high K<sup>+</sup> permeability is due to most cells containing more open K<sup>+</sup> channels (or ‘leak’ channels) at rest as compared to other types of ion channels. At a resting  $V_m$  of -70, neither K<sup>+</sup> nor Na<sup>+</sup> is at electrochemical equilibrium. For K<sup>+</sup>, the negative  $V_m$  that acts to attract K<sup>+</sup> to the intracellular solution is insufficient to balance the chemical force driving K<sup>+</sup> out. A relatively large number of open K<sup>+</sup> channels combined with a small electrochemical driving force result in a continued small efflux of K<sup>+</sup>. For Na<sup>+</sup>, both the negative  $V_m$  and the concentration gradient provide a strong electrochemical driving force for Na<sup>+</sup> influx. However, there are a relative small number of open Na<sup>+</sup> channels and so only a small Na<sup>+</sup> influx occurs. At rest when the  $V_m$  is not changing, we have a steady-state situation, in which the efflux of K<sup>+</sup> is balanced by the influx of Na<sup>+</sup>. Changing the relative membrane permeability will disrupt this delicate balance. Opening of more K<sup>+</sup> channels will allow K<sup>+</sup> efflux to exceed Na<sup>+</sup> influx and  $V_m$  becomes hyperpolarized. Conversely, closing some K<sup>+</sup> channels, or opening of more Na<sup>+</sup> channels, will result in less K<sup>+</sup> efflux or more Na<sup>+</sup> influx, respectively, and a depolarization of the  $V_m$ . Therefore by opening and closing K<sup>+</sup> and/or Na<sup>+</sup> channels, a cell can readily change its membrane potential. Cells also contain ion channels that allow other physiological ions such as Cl<sup>-</sup>, HCO<sub>3</sub><sup>-</sup>, and Ca<sup>2+</sup> to diffuse across the membrane according to their electrochemical gradients. Hence by combining concentration gradients established by active transport mechanisms, and changes in relative membrane permeability by opening and closing an array of different types of ion channels, cells can change the  $V_m$  to a range of different levels and thereby induce and transduce physiologically relevant electrical signals. Such electrical signals include resting membrane potentials, action potentials, synaptic potentials, sensory, and receptor potentials.

### Do Ion Concentrations Change When the $V_m$ Changes?

A logical question to ask regards whether the efflux of K<sup>+</sup> and influx of Na<sup>+</sup> that occurs to establish the resting membrane potential changes the concentration gradients. Similarly with changes in  $V_m$ , such as action potentials and synaptic potentials, will these ion fluxes change the intracellular and extracellular ion concentrations? The answer is that only a relatively small number of ions flow across the membrane to generate the resting  $V_m$  or changes in  $V_m$  associated with action potentials or other membrane potential changes. The intracellular and extracellular concentrations do change, but for Na<sup>+</sup> and K<sup>+</sup> (and most other ions) this does not significantly change the concentration gradients. [Box 3](#) below estimates that a single action potential in a typical nerve cell soma causes an increase in intracellular Na<sup>+</sup> concentration of less than 1 μM, or <0.01% change from a resting concentration of about 18 mM. An even smaller relative change would occur with the efflux of K<sup>+</sup> ions that generates the typical negative resting  $V_m$ . In a small diameter (1 μm) axon, a similar calculation gives a change of 0.2 mM Na<sup>+</sup> during a single action potential. Prolonged high-frequency action potentials may elevate Na<sup>+</sup> significantly in such small spaces (and some nerve axons or processes can be even thinner), although the Na<sup>+</sup> pump is strongly stimulated by intracellular Na<sup>+</sup> to counteract such buildup. During some pathological conditions such as seizures, the high frequency of action

### Box 3 How many ions flow across the membrane to cause a voltage change of 100 mV?

An estimate of this can be done using some biophysical equations and approximated values. We consider the case of a neonatal rat motor neuron, for which we have reliable morphological and electrical data, with a somatic surface area of approximately  $2 \times 10^{-5} \text{ cm}^2$  ( $2000 \mu\text{m}^2$ ) and a total membrane capacitance of about  $40 \text{ pF}$  (Thurbon *et al.*, 1998).

$$\begin{aligned}\text{Charge}(Q) &= \text{Capacitance}(\text{Cm}) \times \text{Voltage}(\text{Vm}) \\ &= 40 \text{ p Farads} \times 100 \text{ mVolts} \\ &= 40 \times 10^{-12} \text{ F} \times 100 \times 10^{-3} \\ &= 4 \times 10^{-12} \text{ Coulombs}(C; 1C = 1 \text{ F.V.})\end{aligned}$$

The charge on a single ion is the elementary charge,  $1.6 \times 10^{-19} \text{ C}$ . Hence  $4 \times 10^{-12} \text{ C} = 4 \times 10^{-12} / 1.6 \times 10^{-19} = 2.5 \times 10^7$  ions.

1 mol of ions =  $6.02 \times 10^{23}$  ions (Avogadro's number) so  $2.5 \times 10^7$  ions =  $4.2 \times 10^{-17}$  mol.

We will consider now that the charge carrier for the 100 mV  $V_m$  change is  $\text{Na}^+$ , coming in to the neuron during an action potential. An efflux of  $\text{K}^+$  to generate a  $-100 \text{ mV}$  resting  $V_m$  would be the same charge movement, but would result in an even smaller relative change in the intracellular  $[\text{K}^+]$  due to the higher resting  $[\text{K}^+]$ .

The surface area (SA) of a sphere is  $4 \times \pi \times r^2$ , the radius ( $r$ ) is  $\frac{1}{2} \times \sqrt{SA/\pi}$  while the volume is  $4/3 \times \pi \times r^3$ . Assuming the soma equates to a sphere (an approximation), and neglecting the dendritic tree (for simplicity) the radius of the neuronal soma is:

$$\begin{aligned}\text{Radius} &= 1/2 \times \sqrt{\left(2 \times 10^{-5} \text{ cm}^2\right)/\pi} \\ &= 2.52 \times 10^{-3} \text{ cm} (\text{or } 25 \mu\text{m}) \\ \text{Volume} &= 4/3 \times \pi \times (2.52 \times 10^{-3} \text{ cm})^3 \\ &= 6.73 \times 10^{-8} \text{ cm}^3 \\ &= 6.73 \times 10^{-8} \text{ ml} \\ &= 6.73 \times 10^{-11} \text{ l}\end{aligned}$$

Hence a 100 mV action potential is an influx of  $4.2 \times 10^{-17}$  mol of  $\text{Na}^+$  into a volume of  $6.73 \times 10^{-11}$  litres. Molar concentration is expressed as moles per litre, so:

$$\begin{aligned}&= 4.2 \times 10^{-17} \text{ mol} / 6.73 \times 10^{-11} \text{ l} \\ &= 0.62 \times 10^{-6} \text{ mol l}^{-1} \\ &= 0.62 \times 10^{-3} \text{ mmol l}^{-1} (\text{mM}) (\approx 0.0006 \text{ mM})\end{aligned}$$

Assuming an intracellular  $\text{Na}^+$  concentration of 12 mM, a 0.0006 mM increase in  $\text{Na}^+$  concentration is an increase of 0.005%, an insignificant change in total concentration.

potentials occurring synchronously in many neurons can also result in significant buildup of extracellular  $\text{K}^+$  (Somjen, 2002). Usually extracellular  $\text{K}^+$  increases will be buffered by surrounding glial cells or diffuse through the extracellular spaces, and saturation of this capacity can have detrimental effects such as helping to further propagate seizures and/or spreading depression (Somjen, 2002). Pathological changes in blood ion concentrations, often a result of kidney dysfunction or as a side effect of diuretics, can also result in changes in electrochemical driving forces and in the membrane potential. Chronic kidney disease, for example, is associated with hyperkalemia that results in chronic peripheral nerve depolarization and alterations in excitability that likely contributes to a range of uremic neuropathy symptoms (Krishnan and Kiernan, 2007).

### Active Ion Transport via Primary and Secondary Active Transporters

For a specific ion to carry its charge across the membrane and change the membrane potential the membrane must be permeable to that ion. The membrane transporters that mediate movement of ions across the membrane fall into two broad categories: active and facilitated diffusion transporters (Table 2). Primary active transporters, such as the sodium pump ( $\text{Na}^+/\text{K}^+$ -ATPase) or the  $\text{Ca}^{2+}$  pump ( $\text{Ca}^{2+}$ -ATPase) directly utilize energy to establish ion concentration gradients. These gradients are used to fuel secondary active transport, in which the movement of one ion species down its electrochemical gradient is coupled to uphill movement of other ion species or solutes against their electrochemical gradient. These secondary transporters, such as the  $\text{K}^+/\text{Cl}^-$  cotransporter or the  $\text{Na}^+/\text{H}^+$  exchanger, can also significantly influence the concentration gradients of ions that contribute to shaping the membrane potential. The  $\text{K}^+/\text{Cl}^-$  cotransporter and the  $\text{Na}^+/\text{K}^+/\text{Cl}^-$  cotransporter are particularly important in determining  $\text{Cl}^-$  concentration gradients, as a primary active transport pump for  $\text{Cl}^-$  does not seem to exist in most cells. Some of these active transporters are 'electrogenic,' that is, they result in a separation of charge across the membrane in each transport cycle. The  $\text{Na}^+$  pump, for example, exports 3  $\text{Na}^+$  ions and imports two  $\text{K}^+$  ions in each transport cycle, utilizing one molecule of ATP in the process. Hence a net movement of 1 positive charge out of the cell occurs in each transport cycle resulting in an increase in negative voltage inside the cell. Blocking the  $\text{Na}^+$  pump using ouabain has been reported to depolarize the  $V_m$  by 2–3 mV, as well as resulting in a gradual build up of intracellular  $\text{Na}^+$  and depletion of intracellular  $\text{K}^+$  (e.g., Thomas, 1972). The modest effects on  $V_m$  of the  $\text{Na}^+$  pump as compared to ion channels relate to the 1000-fold or more lower rates of ion transport through the  $\text{Na}^+$  pump (and other active transporters) as compared to ion channels. Hence their contribution to relative membrane permeability is also minimal. The  $\text{Na}^+$  pump undergoes numerous conformational changes during the transport cycle, binding and trapping  $\text{Na}^+$  and  $\text{K}^+$  and undergoing phosphorylation and dephosphorylation in a series of discrete conformation states. Even when the  $\text{Na}^+$  pump is strongly stimulated, the rate at which it moves  $\text{Na}^+$  or  $\text{K}^+$  across the membrane is of the order of  $10^3$ – $10^4$  ions per second, whereas ion channels can mediate ionic fluxes of at rates of  $10^6$ – $10^8$  ions per second (Hille, 1992). The small contribution that the electrogenic  $\text{Na}^+$  pump contributes to the resting membrane potential can be accounted for by modifying the relative  $\text{Na}^+$  and  $\text{K}^+$  permeability using a coupling coefficient, the parameter  $r$  in eqn [4] (Mullins and Noda, 1963). This coefficient reflects the pumps transport stoichiometry, being  $3/2$  for the  $\text{Na}^+$  pump. Using physiological values of  $\text{Na}^+$  and  $\text{K}^+$  concentrations and relative permeabilities, eqn [4] calculates that the  $\text{Na}^+$  pump contributes a 2.0 mV hyperpolarization to the resting membrane potential.

### Passive Ion Transport via Selective, Facilitated Diffusion Ion Channels

Although primary and secondary active transporters establish and maintain ion gradients, ion channels, being facilitated

**Table 2** Classification and distinguishing characteristics of membrane transport processes

	Passive processes		Active processes				
	Simple diffusion	Facilitated diffusion		Primary active transport	Secondary active transport		
			Carrier	Channel		Cotransport	Counter transport
Alternate name	Lipid diffusion	Diffusion carrier	Channels or pores	Pump	Uniporter	Exchanger	
Energy used	Nil	Nil	Nil	Yes, direct	Yes, indirect	Yes, indirect	
Chemical nature of transported substance	Nonpolar/lipid soluble molecules	Ions or other polar substances	Ions or other polar substances	Ions or other polar substances	Ions or other polar substances	Ions or other polar substances	
Permeation pathway/mechanism	Via the lipid	Via membrane protein	Via membrane protein	Via membrane protein	Via membrane protein	Via membrane protein	
Driving force for solute movement	Chemical (concentration gradient)	Chemical (concentration gradient)	Electrochemical (concentration gradient and electrical force)	ATP hydrolysis fuels uphill solute flux	Solute movement down electrochemical gradient drives another solute uphill in same direction	Solute movement down electrochemical gradient drives another solute uphill in opposite direction	
Example of substances transported	O <sub>2</sub> , CO <sub>2</sub> , steroids	Glucose, amino acids	Na <sup>+</sup> , K <sup>+</sup> , Cl <sup>-</sup> , Ca <sup>2+</sup> , H <sub>2</sub> O	Na <sup>+</sup> , K <sup>+</sup> , Ca <sup>2+</sup> , H <sup>+</sup>	Glucose, amino acids, Cl <sup>-</sup>	Ca <sup>2+</sup> , H <sup>+</sup>	
Example of transporter	Not applicable	GLUT4 glucose transporter	Voltage-dependent Na <sup>+</sup> channel	Na <sup>+</sup> /K <sup>+</sup> /ATPase (Na <sup>+</sup> pump)	GLUT1 glucose transporter	Na <sup>+</sup> /Ca <sup>2+</sup> exchanger	
Example of physiological function	Oxygen flow from blood to cells	Glucose movement into cells following a meal	Generation and propagation of the action potential	Establish and maintain physiological [Na <sup>+</sup> ] and [K <sup>+</sup> ]	Store glucose into liver cells	Intracellular [Ca <sup>2+</sup> ] homeostasis	

diffusion transporters, dissipate these ionic gradients. The study of ion channels has been remarkably advanced over the past two decades by the elucidation of the crystal structure of ion channels from bacteria and other simple organisms which can be grown to yield large quantities of membrane proteins amenable to crystallization. These ion channels have gene sequences and protein structures homologous to our own ion channels, so provide insights into mammalian ion channels. The importance of this work was recognized by the award of the Nobel Prize in chemistry in 2002, to Professors Rod Mackinnon and Peter Agre for their discoveries concerning K<sup>+</sup> channels and water channels, respectively (see Relevant Websites). The structure of the yeast KcsA K<sup>+</sup> channel discovered by Prof Mackinnon's laboratory in 1998 is shown in **Figure 5(a)** (Doyle *et al.*, 1998). It illustrates some of the key structural features of ion channels – a 'selectivity filter' that allows certain ions to pass into the aqueous channel pore but not others, and a 'channel gate' that opens and/or closes in response to certain stimuli and thereby allows different changes in membrane permeability under different physiological conditions.

The selectivity properties of K<sup>+</sup> channels such as the KcsA channel are quite remarkable – they can allow K<sup>+</sup> ions to pass through at high rates of up to 1 million sec<sup>-1</sup> while the very similar and slightly smaller (when dehydrated) Na<sup>+</sup> ion is strongly excluded (the K<sup>+</sup>:Na<sup>+</sup> selectivity of some K<sup>+</sup> channels is 100:1 or more; Hille, 1992; Doyle *et al.*, 1998). Such high selectivity can be achieved as the dehydrated K<sup>+</sup> ion fits perfectly into the somewhat rigid selectivity filter, where it can be momentarily stabilized by interactions with negative dipoles from carbonyl oxygen groups arising from some of the amino acids that form the selectivity filter (**Figure 5(b)**). The energy lost by liberating the hydrating H<sub>2</sub>O molecules can be regained by interactions with the carbonyl oxygens. Na<sup>+</sup> ions, in contrast, cannot interact as closely with the negative dipoles in the selectivity filter (the diameter of a bare Na<sup>+</sup> is slightly smaller than K<sup>+</sup> – 0.09 nm compared to 0.10 nm) and hence prefers to stay hydrated by H<sub>2</sub>O. An important principle of relative ion selectivity is this balance between energy of dehydration and energy of interaction with residues within the selectivity filter. Voltage-dependent Na<sup>+</sup>, K<sup>+</sup>, and Ca<sup>2+</sup> channels are, in general, very highly selective, but other channels have lower selectivity. The synaptic glutamate and acetylcholine receptors can pass both Ca<sup>2+</sup>, Na<sup>+</sup>, and K<sup>+</sup> to various degrees amongst the different subtypes. Nicotinic acetylcholine channels in frog skeletal muscles do not discriminate much amongst monovalent cations and have a relative Ca<sup>2+</sup>:Na<sup>+</sup> permeability of about 0.2 (Adams *et al.*, 1980) while the neuronal α7 subtype is more permeable to Ca<sup>2+</sup> than Na<sup>+</sup> by about 10:1 (Bertrand *et al.*, 1993). Anion channels, such as gamma-aminobutyric acid (GABA) and glycine-receptor channels, are generally also weakly selective amongst different anions, and can even let a small degree of cations to pass through (Keramidas *et al.*, 2004; Franciolini and Nonner, 1987; Sugiharto *et al.*, 2008). Note in the KcsA channel the negatively charged residues surrounding the entrance to the channel pore. This illustrates another common theme in ion channel permeation – charged residues surrounding the entrances to the channel pore can concentrate permeant ions and hence increase the rate at which they can then flow through the channel pore (Moorhouse *et al.*, 2002; Carland *et al.*, 2009). These charged residues may also

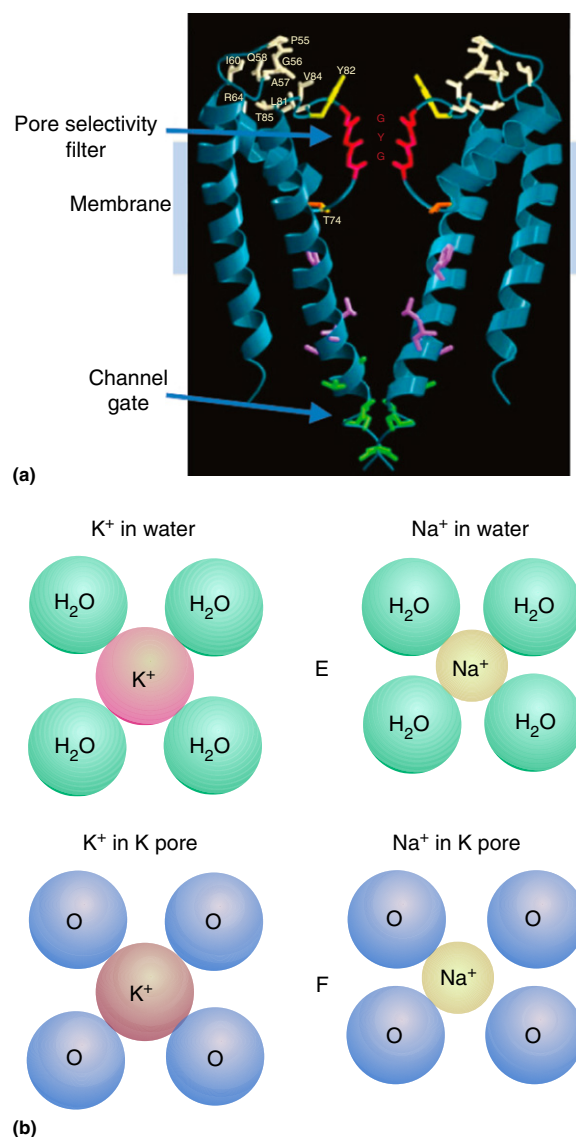


**Figure 5** Structure of a K<sup>+</sup>-selective ion channel. (a) X-ray structure of the bacteria *Streptomyces lividans* KcsA K<sup>+</sup> channel (Doyle *et al.*, 1998). Two adjacent polypeptide subunits (of the four in total) are shown. The two transmembrane alpha-helical segments, and the angled pore-helix, are indicated in blue, some other amino acids are numbered and labeled with their single letter code. Of note is the 'GYG pore selectivity filter' that lines the top of the channel pore, and the 'channel gate' at the intracellular end. Adapted with permission from part of **Figure 4** of Doyle, D.A., Morais, C.J., Pfuetzner, R.A., *et al.*, 1998. The structure of the potassium channel: Molecular basis of K<sup>+</sup> conduction and selectivity. *Science* 280, 69–77. (b) Schematic diagram illustrating energetics of why the larger diameter K<sup>+</sup> ion is selected over the smaller diameter Na<sup>+</sup> ion in the pore of the KcsA K<sup>+</sup> channel (panels C–F of Armstrong, C., 1998. *Science* 280 (5360), 56–57, with permission). Both ions are hydrated and stable when in the extracellular and intracellular solutions (and also in the central cavity of the channel). However, in the restricted region of the selectivity filter, the ions need to be dehydrated to pass through, K<sup>+</sup> 'fits' better in the selectivity filter of Na<sup>+</sup>, as it can be more effectively stabilized by the negative dipole of carbonyl oxygens from the pore structure.

contribute more directly to determining which type of ion – an anion or cation – is preferred through the pore (Keramidas *et al.*, 2002; Cymes and Grosman, 2012).

### **Ion Channel Gating**

**Figure 5(a)** also illustrates the occlusion of the aqueous pore that forms the channel gate. The KcSA structure in **Figure 5(a)** represents a nonconducting state through which no ions can pass. A decrease in the pH of the bacteria cell induces conformational changes that include large opening at the inner end of the membrane domains and that ultimately results in a conducting channel (Liu *et al.*, 2001). For voltage-dependent channels, membrane potential changes are detected by specialized voltage-sensor domains that respond with conformational changes that initiate opening of the channel pore (Bezanilla, 2000). In the cys-loop family of ligand-gated ion channels, the channel gate lies within the transmembrane pore that is more than 50 Å away from the specific ligand-binding domain – yet when the neurotransmitters bind to this site, a conformational wave is initiated that opens the channel in less than 0.1 ms (Sine and Engel, 2006). Membrane stretch is another way of activating channels, as well as being able to change the sensitivity of channels to other forms of gating. Other channels are ‘leaky,’ or open in absence of any particular stimuli. These channels include the  $K^+$  selective channels referred to above in the context of setting the resting membrane potential. Ion channels, however, do not spend all their time in just one conformational state and may spontaneously switch between closed and open conformations. Some resting ‘leak’ channels, for example, the inward rectifying  $K^+$  channels can be gated to either increase or decrease the amount of time spent in the open conformation: binding of G-protein subunits can open channels of the Kir gene family 3, while  $K^+$  channels of the Kir family 6 decrease their open time when ATP levels in cells increase (Reimann and Ashcroft, 1999). Furthermore, channels have multiple gates – voltage-dependent channels, for example, activate in response to a depolarization and then inactivate during sustained depolarization via a second distinct ‘inactivation’ gate that occludes the open pore. This fast inactivation process is important for rapid electrical signaling; toxins or genetic mutations that disrupt the inactivation gate of voltage-dependent  $Na^+$  or  $Cl^-$  channels can result in muscle diseases and epilepsy (Ashcroft, 2000). In an analogous fashion, some ligand activated channels can also transit to a closed conformation in the sustained presence of ligand through a process known as ‘desensitization.’ The precise nature of this desensitization gate remains unknown. Clearly the modes and mechanisms of channel gating are numerous and complex, yet enables changes in membrane permeability at different times in response to different physiological stimuli that result in a myriad of membrane potential changes such as action potentials, synaptic potentials, sensory potentials, and more.

### **Passive Membrane Potential Changes**

The membrane potential changes underlying an action potential, generated in response to sensory stimulation, or arising in response to release of neurotransmitters at a synapse, all involve ionic currents flowing across the membrane through different

ion channels. Membrane potential changes can also occur in the absence of a specific activating stimulus, but rather arise ‘passively’ (although ions also flow passively through channels) or ‘electrotonically’ by conduction between two regions of different potential within the cell. A geometrically simple cell, such as a small and round neuron without much processes, or a red blood cell, is isopotential, meaning that the membrane potential at each point inside the cell is the same. For cells of more complex geometry, such as an elongated muscle cell, a long nerve axon, or a nerve cell with extensive dendritic elongations, the  $V_m$  at one point of the cell can differ from that at other points of the cell. Consider a motoneuron innervating a muscle in the foot: an action potential depolarizes the soma membrane within the ventral horn of the spinal cord, but the neurotransmitter that initiates the muscle response is packaged in a nerve terminal up to 1 m away. When the soma is depolarized by the action potential, the  $V_m$  at the nerve terminal is still at rest, and the depolarization needs to spread along the nerve cell to the terminal to initiate neurotransmission. Similarly, a layer V pyramidal neuron gets depolarized at a distal synapse in a different layer of the cortex, and this  $V_m$  change needs to spread to the soma where an action potential response could potentially result. In both these cases, the  $V_m$  is not the same at these two points in the same cell, creating a potential difference between these two points that drives the movement of charge, or current. Cations will flow along the core of the dendrite or axon from the depolarized region to the more hyperpolarized region (with anions flowing in the opposite direction). As the positive current moves along the cell membrane, it causes a spread of depolarization. This local current flow is ‘passive’ or ‘electrotonic’ propagation, and works just as effectively for the spread of either depolarizations or hyperpolarizations. The distance and speed at which this passive depolarization (or hyperpolarization) is propagated along a cell membrane depends on (1) the amplitude of the difference in potential between the two points, (2) how many ions will ‘leak’ out across the plasma membrane, relative to how many will flow through the core of the axon, dendrite, or other excitable cell, and (3) how quickly will this movement of charge causes a change in the  $V_m$ . **Figure 6** demonstrates the decay of these passive responses as one gets further away from the point at which the membrane is most polarized. **Figure 3** demonstrates how the passive response recorded at a single point in response to a step change in current changes over time. The two key intrinsic or passive properties of the cell membrane that control these temporal and spatial aspects of the membrane potential are the ‘space constant’ and ‘time constant’ – and these can vary markedly across cells of different shapes and sizes. A series of cable equations relate the resistances, capacitances, and geometries of the membrane and interior of a nerve ‘cable’ to the distance and speed a passive propagation can travel (**Figure 6**; see also Aidley, 1989; Boron and Boulpaep, 2009; Byrne, 2015). Over short distances of less than 1 mm, from the membrane of a synaptic cleft to the extrasynaptic membrane in a skeletal muscle, or from one Node of Ranvier to another in a myelinated nerve axon, passive depolarizations can be effective. But they will not suffice to propagate a depolarization in a long motoneuron nor even in a long dendritic tree. For long distance spread of membrane potentials, active depolarizations are required. In nerve axons, local (passive) currents spread the depolarization to an adjacent region

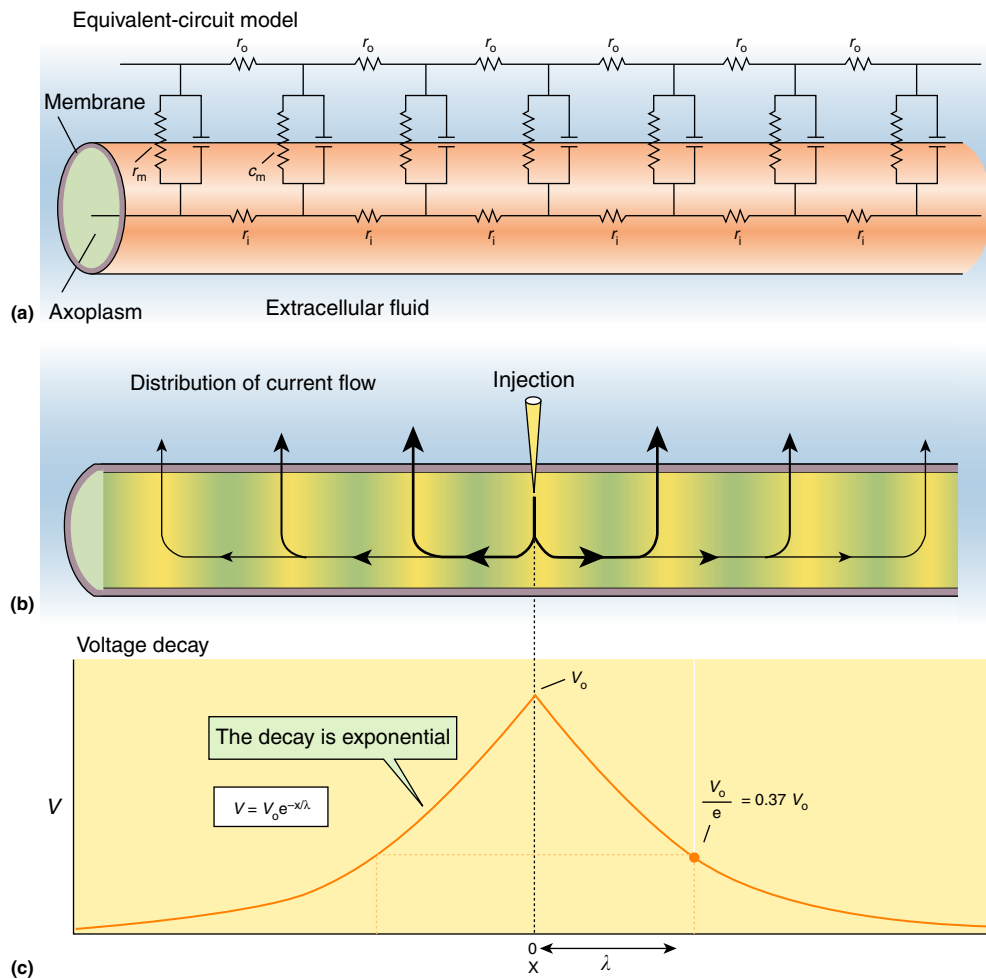


**Figure 6** Passive membrane properties of a cylindrical cell. (a) Schematic diagram of a nerve axon, indicating the equivalent electrical properties of axoplasmic or internal resistance,  $r_i$ , an external resistance ( $r_o$ ), a membrane resistance ( $r_m$ ), and membrane capacitance ( $C_m$ ) (see also Figure 3). These values defined for a unit length of a cylinder or cable can be converted to those of a unit area by incorporating the axon radius,  $a$ , so that  $r_i = R/\pi a^2$  ( $\Omega \text{ cm}^{-2}$ );  $r_m = R_m/2\pi a$  ( $\Omega \text{ cm}^{-2}$ ), and  $C_m = C_m \times 2\pi a$  ( $\mu\text{F cm}^{-2}$ ). (b) As ionic current is injected into a particular point along a cylindrical cell via a microelectrode (or via the opening of an ion channel) the current passively spreads laterally. As the cell membrane is an imperfect insulator, some of the current that was injected 'leaks' across the membrane, meaning that less and less current is available to continue to spread along the axon. (c) A consequence of this leak of current is that the voltage response, or  $V_m$ , exponentially decreases in magnitude as distance from the source of the current increases. The decay depends on the amount of current that stays inside the fibre (or does not leak out), which depends directly on  $r_m$  and inversely on the sum of  $r_i$  and  $r_o$ . One can define a parameter, the space constant,  $\lambda$ , as  $\sqrt{(r_m/r_o + r_i)}$ , and show (e.g., Aidley, 1989, p. 37) that this equals the distance over which the response decays to 37% of its original or peak value ( $V_o$ ). The voltage at distance  $x$ ,  $V = V_o e^{-x/\lambda}$ . As  $r_o \ll r_i$ , one can simplify as  $\lambda = \sqrt{(r_m/r_i)}$ . For a unit area of axon,  $\lambda = \sqrt{(aR_m/2r_i)}$ ; and hence  $\lambda$  increases as axon diameter increases (see Aidley, 1989, p. 38). This is particularly important for the propagation of the action potential along an axon, as the conduction velocity is directly proportional to the  $\lambda$  (and inversely proportional to the time constant  $\tau$ , the product of  $R_m \times C_m$ ). Reproduced from Figure 7.22 in Boron, W.F., Boulpaep, E.L., 2009. Medical Physiology. A Cellular and Molecular Approach, second ed. Philadelphia, PA: Saunders Elsevier. © 2002 Elsevier Science, USA.

where the depolarization crosses a threshold and activates the voltage-dependent  $\text{Na}^+$  and  $\text{K}^+$  channels to regenerate the action potential (that again spreads passively to the next region to be regenerated and so on).

### Measuring Membrane Potential and Relative Membrane Permeability

#### Direct Measurements of Membrane Potential and Membrane Selectivity

The membrane potential is directly measured by inserting an electrode into the inside of a cell and recording the potential

difference between this electrode and one in contact with the solution outside the cell. This was first done for nerve cells by Hodgkin and Huxley (1939) who lowered a wire inside the giant axon of the squid, *Loligo forbesi*, to 1st observe the nerve membrane potential both at rest and in response to stimulation. The experimental approach is shown in a lovely video produced at the Marine Biology Laboratory in the 1970s and posted on youtube (see Section Relevant Websites). A more complete description of this experimental approach and the results was subsequently published in the *Journal of Physiology* (Hodgkin and Huxley, 1945) and is illustrated in Figure 7. The resting  $V_m$  of about  $-50 \text{ mV}$  became positive (about  $+40 \text{ mV}$ ) during

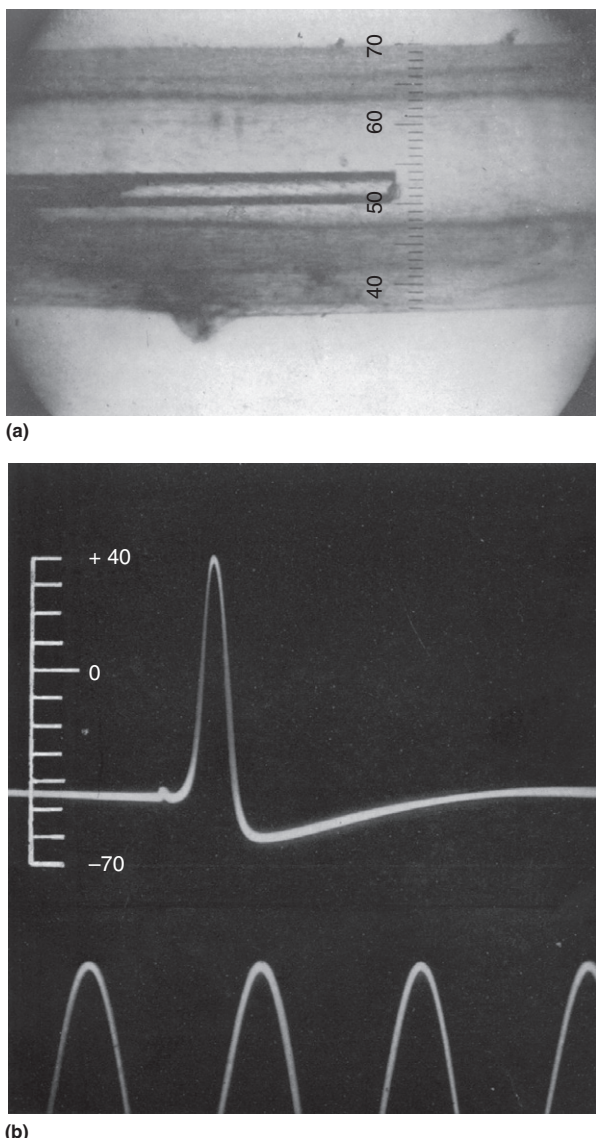


**Figure 7** Direct recording of a nerve membrane potential using an intracellular microelectrode. (a) Photomicrograph of portion of the isolated giant axon of the squid, *Loligo forbesi*, with a 20  $\mu\text{m}$  silver wire enclosed within a  $\approx 100 \mu\text{m}$  glass capillary that is visible inside the  $\approx 0.5 \text{ mm}$  fibre (each small division represents 33  $\mu\text{m}$ ). (b) Direct recording of the  $V_m$  using the configuration shown in (a). The potential difference is between the silver wire microelectrode and a ground electrode connected to the seawater outside the nerve. The y axis is in mV, the time marker is cycles at 500 Hz (or 1 peak per 2 ms). Reproduced with permission from panel a, Plate 1 and Plate 2 of Hodgkin, A.L., Huxley, A.F., 1945. Resting and action potentials in single nerve fibres. *Journal of Physiology* 104, 176–195.

the action potential – this observation that the  $V_m$  overshot zero revealed important insights into the mechanisms of the action potential. Their subsequent application of the voltage-clamp technique, coupled with rigorous and thoughtful analysis, elucidated the basic biophysical mechanisms of the resting and action potential in nerve axons. They provided a highly influential quantitative description of the membrane potential

changes in terms of changes in the membrane conductances to  $\text{Na}^+$  and  $\text{K}^+$ , and the relative membrane permeabilities of the membrane to these ions. On the 50th anniversary of the publication of a series of five seminal papers in the *Journal of Physiology* (1952), a special celebratory issue was published that describes the impact and legacy of their contribution (see Section Relevant Websites).

Using this intracellular recording wire electrode and squid axons, Hodgkin and Katz (1949; also analyzing earlier data of Curtis and Cole) investigated how the resting  $V_m$  and the peak amplitude of the action potential varied as a function of external  $\text{K}^+$  and  $\text{Na}^+$ . They demonstrated that the resting  $V_m$  was sensitive to  $\text{K}^+$  changes but not  $\text{Na}^+$  changes, and vice versa for the  $V_m$  at the peak of the action potential. Fitting the data to the GHK equation gave relative permeabilities,  $P_{\text{K}}/P_{\text{Na}}$ , of about 25:1 for the resting  $V_m$ , and about 1:20 for the peak of the action potential. However, mammalian cells are much smaller than these giant squid axons and not amenable to insertion of a fine wire. Using instead a sharp glass micro-electrode (with a tip of  $<0.1 \mu\text{m}$ ), Hodgkin and Horowicz (1959) conducted similar experiment on isolated skeletal muscle fibers of the frog, measuring resting  $V_m$  and changing the external  $\text{K}^+$ ,  $\text{Na}^+$ , and  $\text{Cl}^-$  concentration in various combinations. The resting  $V_m$  was similarly highly dependent on external  $\text{K}^+$ , with a linear relationship over most of the concentration ranges tested, but with a clear deviation from this relationship at lower extracellular  $\text{K}^+$  (see their data in Figure 8). This deviation is consistent with the membrane being not only permeable to just  $\text{K}^+$ , and fitting the data to the GHK equation gave a  $P_{\text{Na}}/P_{\text{K}}$  of 0.01 for the resting  $V_m$  (Figure 8). When the external  $[\text{K}^+]$  is low, the  $V_m$  is very hyperpolarized so that the electrochemical gradient for  $\text{Na}^+$  influx is very strong (while that for  $\text{K}^+$  is very weak), and the deviation occurs because we now see a significant effect of the  $\text{Na}^+$  influx on  $V_m$  despite the low relative  $\text{Na}^+$  permeability. This work also appreciated (and quantified) that muscle had a high resting  $\text{Cl}^-$  conductance and permeability, but that the steady-state  $V_m$  was independent of changes in  $[\text{Cl}^-]$  (Hodgkin and Horowicz, 1959). This seeming contradiction arises because  $\text{Cl}^-$  is not actively transported across the membrane of skeletal muscle and therefore distributes its concentration gradient passively with  $V_m$  so that  $E_{\text{Cl}}=V_m$ . When muscle  $V_m$  changes, the high  $\text{Cl}^-$  conductance of muscle plays an important role in reducing the extent of  $V_m$  changes and stabilizing muscle excitability. During an action potential, for example,  $\text{Cl}^-$  influx into the depolarized muscle is important for repolarization. Indeed, recessive or dominant mutations in the major human skeletal muscle  $\text{Cl}^-$  channel (CLC1) can cause severe muscle diseases known as generalized myotonia (Becker's disease) and myotonia congenita (Thomsen's disease), respectively (Ashcroft, 2000).

#### Quantifying Membrane and Ion Channel Selectivity Using Voltage-Clamp

In neurons, where active transporters for  $\text{Cl}^-$  typically exist (e.g., KCC2 and NKCC1),  $\text{K}^+$ ,  $\text{Na}^+$ , and  $\text{Cl}^-$  (and to some extent other ions such as  $\text{Ca}^{2+}$  and  $\text{HCO}_3^-$ ) all contribute to the  $V_m$ . The extent to which they do so varies considerably – as the membrane permeability to these ions is constantly

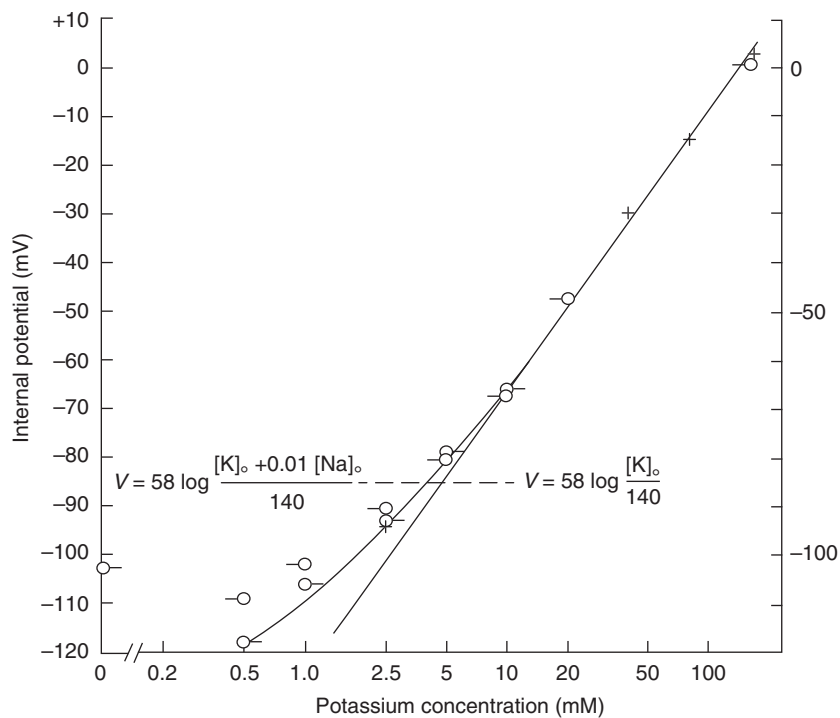


**Figure 8** Quantifying the relative permeability of the cell membrane at rest. Direct recording of the resting  $V_m$  of frog skeletal muscle using an intracellular microelectrode, and the dependence of this resting  $V_m$  on the concentration of  $K^+$  in the external solution. The experimental data points at different times after solution change (and/or after decreases and increases in  $K^+$ ) are given by the open circles and crosses. This data is fit by the Nernst equation (right straight line) and by the GHK equation (left curved line). The better fit is obtained with the GHK equation assuming a relative  $P_{Na}/P_K$  value of 0.01. Reproduced with permission from Figure 5 of Hodgkin, A.L., Horowitz, P., 1959. The influence of potassium and chloride ions on the membrane potential of single muscle fibres. Journal of Physiology 148, 127–160.

changing. Knowing what ion channels are opened by different stimuli, and the ion selectivity properties of these channels – that together determines the membrane permeability – is an important aspect of understanding and predicting the different types of membrane potential changes seen *in vivo*. Measuring the ionic selectivity of a specific ion channel, or of the membrane as a whole, involves the same basic experimental approach as illustrated by the early recordings of Hodgkin, Huxley, and their contemporaries – changing the external solutions and measuring the  $V_m$ . However, this is more precisely done using the voltage-clamp technique. Direct  $V_m$  measurements can be complicated by the fact that changes in the membrane potential can themselves change the channels that are open or the driving forces for ion movement. Greater experimental control is achieved using voltage-clamp recordings – an experimental approach where one controls the voltage by using a feedback amplifier to inject positive or negative current into the cell. The experimenter therefore controls the voltage and measures the current flowing through any channels open at that voltage. To apply to selectivity measurements, one first records the voltage at which no ionic currents flow across the membrane, the current reversal potential ( $V_{rev}$ ), and then changes the solutions on one side of the membrane, and measures the new  $V_{rev}$ . The  $V_{rev}$  is the voltage where the ionic currents are at equilibrium. With knowledge of the ionic composition of the solutions, one can calculate the relative permeability of the membrane using the GHK equation as described above. If a single ion channel is responsible for the

current being measured (either because it has been over-expressed in a cultured cell, or because it has been selectively activated), then these relative permeability measurements correspond to the selectivity properties of the channel itself. Good solution and voltage control, and accounting for various voltage offsets inherent in these recordings (such as liquid junction potentials) is needed to accurately quantify membrane or channel selectivity. Using ionic activities (rather than concentrations) is particularly important when the control and test solutions have different ionic strengths, such as in dilution potential experiments often used to quantify selectivity. The procedures to accurately measure and quantify membrane selectivity are described in more detail elsewhere (Barry, 2006; Sugiharto *et al.*, 2008; 2010; Moorhouse *et al.*, in press), and the results from such an experiment are illustrated in Figure 9.

#### Caveats in Measuring Physiological $V_m$

Use of a microelectrode or patch clamp pipette to measure the potential difference between electrodes inside and outside of the cell is a direct and simple way to measure the membrane potential, but is associated with a number of limitations. Inserting a sharp microelectrode through the cell membrane causes some damage or holes through the membrane. These holes are nonselective ‘leak’ conductances that will change the composition of the cell and thereby potentially affect  $V_m$ . In hippocampal neurons, this damage-induced leak

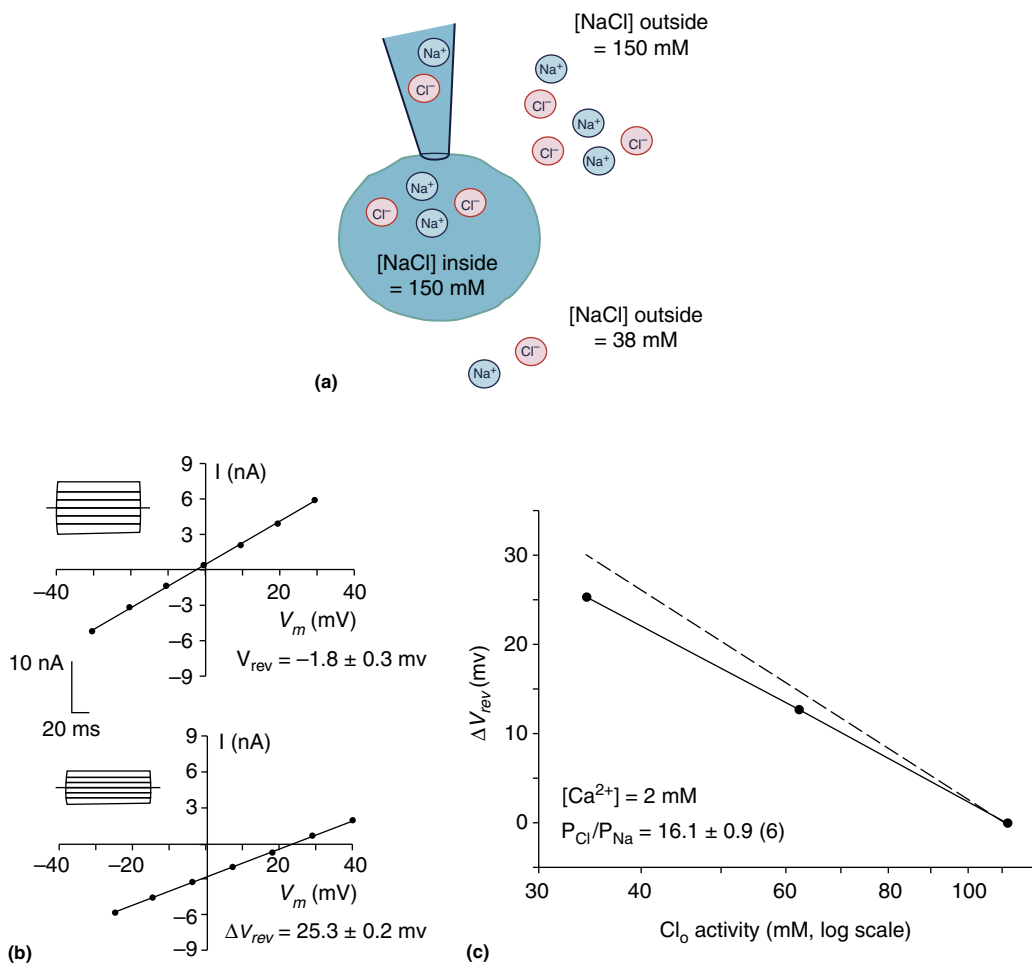


**Figure 9** Quantifying ion channel selectivity using whole-cell patch clamp recordings. (a) Schematic diagram of the whole-cell patch clamp recording that allows the cell to be perfused with an intracellular solution of known ionic concentration, in this case largely 150 mM NaCl. The external solution can also be controlled, and changed from a symmetrical 150 mM NaCl (upper) to a 25% diluted solution (containing 38 mM NaCl; lower). The cell can also be voltage-clamped by the patch clamp configuration, allowing the experimenter to control the  $V_m$  and record the currents flowing across the membrane. (b) Example of glycine-receptor activated ionic currents recorded at different membrane potentials using whole-cell configuration as in (a), in symmetrical (upper) and in 25% dilution NaCl solutions (lower). The graphs plot these  $V_m$  vs. current,  $I$ - $V$ , relationships with the averaged  $V_m$  at which the current was zero ( $V_{rev}$ s) shown in the two graphs. (c) The averaged shift in  $V_{rev}$  as external NaCl is diluted to 50% and then 25% across six different cells is plotted against the external Cl activity, and fit with the GHK equation to obtain a  $P_{Cl}/P_{Na}$  value of about 12 for the recombinant human  $\alpha 1$  glycine receptor. For further detail see Sugiharto *et al.* (2010). As the external NaCl is diluted, a chemical gradient is created for efflux of both Na<sup>+</sup> and Cl<sup>-</sup>. As the GlyR is more permeant to Cl<sup>-</sup>, a positive  $V_m$  is needed to counterbalance this chemical force, and hence  $V_{rev}$  shifts to positive values. A negative shift is seen if  $P_{Na} > P_{Cl}$ . Panels (b) and (c) have been published in different formats as parts of Figures 1 and 2 in Sugiharto *et al.* (2010).

causes the subsequent activation of ion channel conductances that reverse near the resting  $V_m$ , hence the cell's resting input resistance is changed, but there is not so much change in the resting  $V_m$  (Staley *et al.*, 1992; Spruston and Johnston, 1992). This damage is minimized with patch clamp recordings in which the membrane is sealed against a glass pipette, rather than the membrane pierced by the pipette. The resting cell input resistance (a measure of such 'leak') is 3–10-fold higher when the same neuron is recorded using patch clamp electrodes as compared to sharp microelectrodes (Staley *et al.*, 1992; Spruston and Johnston, 1992). So in this respect, a more physiological  $V_m$  value could be obtained with patch clamp recordings. A caveat with both patch clamp and sharp

microelectrodes is that ions leaking from the recording pipette into the cell will change the intracellular ionic composition and hence the physiological  $V_m$ . While this is much more significant for large patch clamp electrodes or sharp microelectrodes, it can be better defined with patch electrodes. Indeed in standard whole-cell patch clamp recordings, the cell interior is almost completely (with time) dialysed by the pipette solution, so one can try to replicate the ionic concentrations and include other constituents to match the physiological milieu as close as possible. Perforated patch clamp recordings can maintain more closely the physiological ion concentrations. This variant of patch clamp recording typically uses different antibiotics inside the pipette solution that forms membrane pores with

permeability limited to ions within a restricted size or polarity, thereby enabling electrical continuity with the intracellular solution while maintaining the physiologically relevant signaling molecules and other larger constituents (Ishibashi *et al.*, 2012). Gramicidin perforated patch, for example, are impermeable to anions and hence have been useful for recording physiological responses to Cl-selective ion channels such as GABA and glycine-activated receptor-channels. While perforated patch can reduce inaccuracies in measuring physiological  $V_m$  related to disrupted intracellular cytoplasm, the technique is associated with a poorly defined voltage offset, relating to the fact that the larger charged molecules left inside the cell may not be properly balanced by charges inside the pipette solution (Horn and Marty, 1988). The liquid junction potential arising from the interface between pipette and bath solutions during the patch clamp procedure, that is between 3–8 mV with typical experimental solutions, must also be taken into account (Barry and Lynch, 1991). Furthermore, one must also appreciate that the voltage-clamp technique can only accurately control the membrane voltage of the membrane isopotential with the pipette – such as the soma in a neuron, while distal regions of cells with complex geometry – such as neuronal dendrites – are less-well controlled, particularly when the voltage or currents across the membrane are rapidly changing (Spruston *et al.*, 1993). Finally, much of our data on membrane potentials comes from *in vitro* conditions where tissues are more readily accessible and solutions and voltage more easily controlled, one must also appreciate that this situation may be quite different from *in vivo* recordings. Indeed, the  $V_m$  fluctuates much more widely in *in vivo* conditions, with much more influences of synaptic and neural circuit activity.

### Physiological Values of $V_m$

Despite the caveats above, one should not be discouraged from measuring directly  $V_m$  using electrophysiological approaches – it is after all a necessary step in quantifying and understanding brain and body function and mechanisms. Using electrophysiological approaches, a wide range of resting  $V_m$  values have been reported for neurons (Table 3). Some of this variability may be technical: for example, Tzyio *et al.* (2003) have demonstrated that in small-sized neurons, a lower resistance pipette-neuron seal, and the procedure of going whole-cell can both depolarize the  $V_m$  somewhat. Avoiding this using a cell-attached variant gave a resting  $V_m$  of about –77 mV, both *in vitro* and *in vivo* (Tzyio *et al.*, 2003, 2008). However, even more hyperpolarized resting  $V_m$  have been reported using standard patch clamp recordings, suggesting minimal artifactual depolarizations in these studies (Table 3). Table 3 is populated with studies where  $V_m$  has been recorded in the same conditions but for different experimental techniques. A number of noteworthy points are: (1) the  $V_m$  can vary markedly in different cell types, both *in vitro* and *in vivo* (e.g., 15 mV difference in averaged  $V_m$  of mitral cells and granule cells within the olfactory bulb), (2) there seems little effect of age and preparation type when  $V_m$  is recorded using the same conditions (e.g., Tzyio *et al.* papers report approximately the same  $V_m$  value in slices, in culture, *in vivo*, and across development), and (3) the results reported by different groups using the same preparation can vary. The variability seems particularly large *in vivo*, perhaps not surprising considering the large spontaneous  $V_m$  fluctuations reported. In the somatosensory

**Table 3** Some reported resting neuronal  $V_m$  values, recorded under different conditions to illustrate potential sources of variability

Neuron type	Preparation	Technique	$V_m$	Reference
<i>In vitro</i>				
Hippocampus DG <sup>a</sup>	Brain slice	WC <sup>c</sup> patch clamp	–84 ± 1.0 (31)	Staley <i>et al.</i> (1992)
Hippocampus DG	Brain slice	Sharp Microelectrode	–74 ± 2.1 (11)	Staley <i>et al.</i> (1992)
Hippocampus CA1	Brain slice	Perforated patch	–64 ± 2 (12)	Spruston and Johnston (1992)
Hippocampus CA3	Brain slice	Perforated patch	–66 ± 1 (12)	Spruston and Johnston (1992)
Hippocampus DG	Brain slice	Perforated patch	–74 ± 2 (12)	Spruston and Johnston (1992)
Hippocampus CA3	Brain slice P2	Perforated patch	–48 ± 3 (6)	Tzyio <i>et al.</i> (2003)
Hippocampus CA3	Brain slice P13–14	Perforated patch	–67 ± 2 (12)	Tzyio <i>et al.</i> (2003)
Hippocampus CA3	Brain slice P2	Cell-attached patch	–77 ± 2 (9)	Tzyio <i>et al.</i> (2003)
Hippocampus CA3	Brain slice P13–14	Cell-attached patch	–77 ± 2 (6)	Tzyio <i>et al.</i> (2003)
Hippocampus CA3	Cultured neurons, 16–21 days	Cell-attached patch	–76 ± 2 (8)	Tzyio <i>et al.</i> (2008)
Hippocampus CA3	Brain slice P2–3, 5 GΩ seal	WC patch clamp	–50 ± 3 (10)	Tzyio <i>et al.</i> (2003)
Hippocampus CA3	Brain slice P2–3, 14 GΩ seal	WC patch clamp	–65 ± 3 (10)	Tzyio <i>et al.</i> (2003)
Hippocampus CA3	Cultured neurons, 16–21 days	WC patch clamp	–56 ± 3 (72)	Tzyio <i>et al.</i> (2008)
<i>In vivo</i> <sup>b</sup>				
Thalamic neurons (VPML)	<i>In vivo</i> , anaesthetized	WC patch clamp	–65.1 ± 4.3 (31)	Margrie <i>et al.</i> (2002)
Layer 4 cortex	<i>In vivo</i> , anaesthetized	WC patch clamp	–81.8 ± 6.3 (23)	Margrie <i>et al.</i> (2002)
Layer 2/3 cortex (excitatory)	<i>In vivo</i> , anaesthetized	WC patch clamp	–83.8 ± 5.2 (31)	Margrie <i>et al.</i> (2002)
Layer 2/3 cortex (excitatory)	<i>In vivo</i> , awake (quiet)	WC patch clamp	–58 ± 1 (32)	Gentet <i>et al.</i> (2010)
Layer 2/3 cortex (inhibitory)	<i>In vivo</i> , awake (quiet)	WC patch clamp	–52 ± 1 (62) <sup>d</sup>	Gentet <i>et al.</i> (2010)
Olfactory bulb granule cells	<i>In vivo</i> , anaesthetized	WC patch clamp	–72 ± 2 (42)	Margrie <i>et al.</i> (2002)
Olfactory bulb mitral cells	<i>In vivo</i> , anaesthetized	WC patch clamp	–57 ± 2 (48)	Margrie <i>et al.</i> (2002)

<sup>a</sup>Hippocampal subfields as dentate gyrus (DG) and Cornu Ammonis (CA) 1 and 3.

<sup>b</sup>*In vivo* during quiet wakefulness, average of both the up and down states but during relative nonspiking periods;

<sup>c</sup>WC = whole-cell.

<sup>d</sup>This value combines the reported  $V_m$  for fast spiking and nonfast spiking groups.

cortex of the awake, behaving mouse, the 'resting'  $V_m$  oscillates at a frequency of 1–5 Hz and with an amplitude of up to 20 mV (Poulet and Petersen, 2008; Gentet *et al.*, 2010). During active behaviors, such as whisking, the  $V_m$  oscillations in corresponding cortical neurons are reduced and the baseline  $V_m$  becomes a few mV more depolarized (Poulet and Petersen, 2008). Averaging the  $V_m$  fluctuations over a few seconds gives values of  $-60$  mV to  $-50$  mV, but the exact value depends very much on the oscillation frequency and the brain state when recordings are measured. Furthermore, the frequency and amplitude of the currents responsible for these oscillations are markedly affected by different anesthetics (Doi *et al.*, 2007). Indeed, the concept of a 'resting  $V_m$ ' is perhaps meaningless for some types of neurons *in vivo*, highlighting the dynamic nature of neuronal activity that can be obscured *in vitro*.

In summary, one cannot give a uniform and single answer to 'What is the resting  $V_m$ ?' In neurons, it may be as depolarized as  $-50$  mV, and as hyperpolarized as  $-85$  mV. In less dynamic and more homogeneous cell types, it may be more consistent. *In vivo*,  $V_m$  may never be 'resting.' Clearly it depends on the region examined, but can also be affected by the recording approach. With careful consideration of voltage offsets, solutions and other potential caveats described above, measurements can provide good estimates of physiological  $V_m$ . While caution is needed in comparing across different conditions, changes in  $V_m$  induced by some physiological or experimental manipulation can be quite valid and informative.

## Conclusion

This article provides an overview of the membrane potential – the polarization of cell membranes arising from a different distribution of ionic charges between the intracellular and extracellular surface of the cell membrane. Some physical and chemical properties of the ions and the membrane were introduced. The lipid nature of the membrane provides an energetically high barrier to passage of hydrated ions, making it a good separator of charge. Active transporters use energy, directly or indirectly, to establish ion concentration gradients and to move ions and other solutes against their energy gradients. Ions can rapidly cross the membrane via ion channels that contain integral membrane pores allowing ions to move passively down their electrochemical gradients. Ion channels have selectivity filters that control the flow of ions across the membrane, and gates that can be opened and closed in response to different physiological stimuli. The nature and number of ions channels open gives rise to the selectivity of the membrane for particular ions, and it is the combination of the relative membrane selectivity to different ions and the electrochemical driving force for each ion that sets the membrane potential at any particular time. Quantifying the relative selectivity of the membrane, or of individual channels, is a key component of understanding the molecular and cellular mechanisms of membrane potentials – this can be readily undertaken but one must be aware of various caveats and offsets involved in such measurements. Similarly, careful consideration is needed to accurately measure membrane potentials. However, perseverance to quantify and understand ion selectivity and membrane potentials will be rewarded, as changes in  $V_m$  are the primary means by which

cells mediate their function and communicate and coordinate with other cells in our body.

## Acknowledgments

Research in the author's laboratory referred to above has been gratefully funded by UNSW Faculty Research Grants, the Australian Research Council, and the National Health and Medical Research Council of Australia. The author thanks Professor Peter Barry for helpful discussions and for the kind permission to use his schematic in Figure 3(b).

## References

- Aidley, D.J., 1989. Physiology of Excitable Cells, third ed. Cambridge: Cambridge University Press.
- Adams, D.J., Dwyer, T.M., Hille, B., 1980. The permeability of endplate channels to monovalent and divalent metal cations. *Journal of General Physiology* 75, 493–510.
- Ashcroft, F.M., 2000. Ion Channels and Diseases. San Diego, CA: Academic Press.
- Barry, P.H., 2006. The reliability of relative anion-cation permeabilities deduced from reversal (dilution) potential measurements in ion channel studies. *Cell Biochemistry and Biophysics* 46, 143–154.
- Barry, P.H., Lewis, T.M., Moorhouse, A.J., 2013. An optimised 3 M KCl salt-bridge technique used to measure and validate theoretical liquid junction potential values in patch-clamping and electrophysiology. *European Biophysics Journal* 42, 631–646.
- Barry, P.H., Lynch, J.W., 1991. Liquid junction potentials and small cell effects in patch-clamp analysis. *Journal of Membrane Biology* 121, 101–117.
- Bertrand, D., Galzi, J.-L., Devillers-Thiéry, A., Bertrand, S., Changeux, J.-P., 1993. Mutations at two distinct sites within the channel domain M2 alter calcium permeability of neuronal a7 nicotinic receptor. *Proceedings of the National Academy of Sciences of the United States of America* 90, 6971–6975.
- Bezanilla, F., 2000. The voltage sensor in voltage-dependent ion channels. *Physiological Reviews* 80, 555–592.
- Boron, W.F., Boulpaep, E.L., 2009. Medical Physiology. A Cellular and Molecular Approach, second ed. Philadelphia, PA: Saunders Elsevier.
- Byrne, J.H., 2015. Changes in the spatial distribution of charge. *Neuroscience* (Chapter 3) Online. Available at: <http://neuroscience.uth.tmc.edu/s1/chapter03.html> (accessed 10.02.15).
- Carland, J.E., Cooper, M.A., Sugiharto, S., *et al.*, 2009. Characterization of the effects of charged residues in the intracellular loop on ion permeation in alpha1 glycine receptor channels. *Journal of Biological Chemistry* 284, 2023–2030.
- Coster, H.G.L., 2003. The physics of cell membranes. *Journal of Biological Physics* 29, 363–399.
- Coster, H.G.L., 2009. Discovery of "punch-through" or membrane electrical breakdown and electroporation. *European Biophysics Journal* 39, 185–189.
- Cymes, G.D., Grosman, C., 2012. Tunable pKa values and the basis of opposite charge selectivities in nicotinic-type receptors. *Nature* 474, 526–530.
- Doi, A., Mizuno, M., Katafuchi, T., *et al.*, 2007. Slow oscillation of membrane currents mediated by glutamatergic inputs of rat somatosensory cortical neurons: *In vivo* patch-clamp analysis. *European Journal of Neuroscience* 26, 2565–2575.
- Doyle, D.A., Morais Cabral, J., Pfuetzner, R.A., *et al.*, 1998. The structure of the potassium channel: Molecular basis of  $K^+$  conduction and selectivity. *Science* 280, 69–77.
- Farrant, M., Kaila, K., 2007. The cellular, molecular and ionic basis of GABA(A) receptor signalling. *Progress in Brain Research* 160, 59–87.
- Franciolini, F., Nonner, W., 1987. Anion and cation permeability of a chloride channel in rat hippocampal neurons. *Journal of General Physiology* 90, 453–478.
- Gentet, L.J., Avermann, M., Matyas, F., Staiger, J.F., Petersen, C.C., 2010. Membrane potential dynamics of GABAergic neurons in the barrel cortex of behaving mice. *Neuron* 65, 422–435.
- Henneman, E., Somjen, G., Carpenter, D.O., 1965. Functional significance of cell size in spinal motoneurons. *Journal of Neurophysiology* 28, 560–580.
- Hille, B., 1992. Ionic Channels of Excitable Membranes, second ed. Sunderland, MA: Sinauer.
- Hodgkin, A.L., Horowicz, P., 1959. The influence of potassium and chloride ions on the membrane potential of single muscle fibres. *Journal of Physiology* 148, 127–160.

- Hodgkin, A.L., Huxley, A.F., 1939. Action potentials recorded from inside a nerve fibre. *Nature* 144, 710–711.
- Hodgkin, A.L., Huxley, A.F., 1945. Resting and action potentials in single nerve fibres. *Journal of Physiology* 104, 176–195.
- Hodgkin, A.L., Katz, B., 1949. The effect of sodium ions on the electrical activity of giant axon of the squid. *Journal of Physiology* 108, 37–77.
- Horn, R., Marty, A., 1988. Muscarinic activation of ionic currents measured by a new whole-cell recording method. *Journal of General Physiology* 92, 145–159.
- Ishibashi, H., Moorhouse, A.J., Nabekura, J., 2012. Perforated patch clamp technique. In: Okada, Y. (Ed.), *Patch Clamp Techniques: From Beginning to Advanced Protocols*. Springer Protocols Handbooks Series. Berlin Heidelberg: Springer-Verlag, pp. 71–83. (Chapter 4).
- Kaplan, J.H., 2002. Biochemistry of Na<sub>x</sub>-K<sub>y</sub>-ATPase. *Annual Review of Biochemistry* 71, 511–535.
- Keramidas, A., Moorhouse, A.J., Pierce, K.D., Schofield, P.R., Barry, P.H., 2002. Cation-selective mutations in the M2 domain of the inhibitory glycine receptor channel reveal determinants of ion-charge selectivity. *Journal of General Physiology* 119, 393–410.
- Keramidas, A., Moorhouse, A.J., Schofield, P.R., Barry, P.H., 2004. Ligand-gated ion channels: Mechanisms underlying ion selectivity. *Progress in Biophysics and Molecular Biology* 86, 161–204.
- Krishnan, A.V., Kiernan, M.C., 2007. Uremic neuropathy: Clinical features and new pathophysiological insights. *Muscle Nerve* 35, 273–290.
- Liu, Y.S., Sompornpisut, P., Perozo, E., 2001. Structure of the KcsA channel intracellular gate in the open state. *Nature Structural & Molecular Biology* 8, 883–887.
- Margrie, T.W., Brecht, M., Sakmann, B., 2002. In vivo, low-resistance, whole-cell recordings from neurons in the anaesthetized and awake mammalian brain. *Pflügers Archives* 444, 491–498.
- McCormick, D.A., 2008. Membrane potential and action potential. In: Squire, L.A., et al. (Eds.), *Fundamental Neuroscience*, third ed. San Diego, CA: Elsevier Press (Chapter 6).
- Moorhouse, A.J., Keramidas, A., Zaykin, A., Schofield, P.R., Barry, P.H., 2002. Single channel analysis of conductance and rectification in cation-selective, mutant glycine receptor channels. *Journal of General Physiology* 119, 411–425.
- Moorhouse, A.J., Lewis, T.M., Barry, P.H., in press. Analysing ion permeation in channels, pumps and transporters using patch clamp recording. In: Clark, R.J., Khalid, M.A.A. (Eds.), *Pumps, Channels and Transporters: Methods of Functional Analysis*. NJ: John Wiley & Sons.
- Mullins, L.J., Noda, K., 1963. The influence of sodium-free solutions on the membrane potential of frog muscle fibres. *Journal of General Physiology* 47, 117–132.
- Poulet, J.F., Petersen, C.C., 2008. Internal brain state regulates membrane potential synchrony in barrel cortex of behaving mice. *Nature* 454, 881–885.
- Reimann, F., Ashcroft, F.M., 1999. Inwardly rectifying potassium channels. *Current Opinion in Cell Biology* 11, 503–508.
- Sine, S.M., Engel, A.G., 2006. Recent advances in Cys-loop receptor structure and function. *Nature* 440, 448–455.
- Somjen, G.G., 2002. Ion regulation in the brain: Implications for pathophysiology. *Neuroscientist* 8, 254–267.
- Spruston, N., Jaffe, D.B., Williams, S.H., Johnston, D., 1993. Voltage- and space-clamp errors associated with the measurement of electrotonically remote synaptic events. *Journal of Neurophysiology* 70, 781–802.
- Spruston, N., Johnston, D., 1992. Perforated patch-clamp analysis of the passive membrane properties of three classes of hippocampal neurons. *Journal of Neurophysiology* 67, 508–529.
- Staley, K.J., Otis, T.S., Mody, I., 1992. Membrane properties of dentate granule cells: Comparison of sharp microelectrode and whole-cell recordings. *Journal of Neurophysiology* 67, 1346–1358.
- Sugiharto, S., Carland, J.E., Lewis, T.M., Moorhouse, A.J., Barry, P.H., 2010. External divalent cations increase anion–cation permeability ratio in glycine receptor channels. *Pflügers Archiv: European Journal of Physiology* 460, 131–152.
- Sugiharto, S., Lewis, T.M., Moorhouse, A.J., Schofield, P.R., Barry, P.H., 2008. Anion–cation permeability correlates with hydrated counterion size in glycine receptor channels. *Biophysical Journal* 95, 4698–4715.
- Thomas, R.C., 1972. Intracellular sodium activity and the sodium pump in snail neurones. *Journal of Physiology* 220, 55–71.
- Thurbon, D., Lüscher, H.-R., Hofstetter, T., Redman, S.J., 1998. Passive electrical properties of ventral horn neurons in rat spinal cord slices. *Journal of Neurophysiology* 79, 2485–2502.
- Tyizio, R., Ivanov, A., Bernard, C., et al., 2003. Membrane potential of CA3 hippocampal pyramidal cells during postnatal development. *Journal of Neurophysiology* 90, 2964–2972.
- Tyizio, R., Minlebaev, M., Rheims, S., et al., 2008. Postnatal changes in somatic gamma-aminobutyric acid signalling in the rat hippocampus. *European Journal of Neuroscience* 27, 2515–2528.

## Relevant Websites

- [www.nobel.org](http://www.nobel.org)  
Nobel Organizations.  
[http://onlinelibrary.wiley.com/journal/10.1111/\(ISSN\)1469-7793/homepage/celebrating\\_the\\_work\\_of\\_alan\\_hodgkin\\_and\\_andrew\\_huxley.htm](http://onlinelibrary.wiley.com/journal/10.1111/(ISSN)1469-7793/homepage/celebrating_the_work_of_alan_hodgkin_and_andrew_huxley.htm)  
John Wiley & Sons, Inc.  
<http://www.youtube.com/watch?v=k48XZFGMc8>